Review

Deep-Learning-Based Computer-Aided Systems for Breast Cancer Imaging: A Critical Review

Yuliana Jiménez-Gaona [1,2,3,*], María José Rodríguez-Álvarez [2] and Vasudevan Lakshminarayanan [3,4,*]

[1] Departamento de Química y Ciencias Exactas, Universidad Técnica Particular de Loja,
San Cayetano Alto s/n CP1101608, Loja, Ecuador

[2] Instituto de Instrumentacion para la Imagen Molecular I3M, Universitat Politécnica de Valencia,
E-46022 Valencia, Spain; mjrodri@i3m.upv.es

[3] Theoretical and Experimental Epistemology Lab, School of Optometry and Vision Science,
University of Waterloo, Waterloo, ON N2L3G1, Canada

[4] Department of Systems Design Engineering, Physics, and Electrical and Computer Engineering,
University of Waterloo, Waterloo, ON N2L3G1, Canada

* Correspondence: ydjimenez@utpl.edu.ec (Y.J.-G.); vengulak@uwaterloo.ca (V.L.)

Abstract: This paper provides a critical review of the literature on deep learning applications in breast tumor diagnosis using ultrasound and mammography images. It also summarizes recent advances in computer-aided diagnosis/detection (CAD) systems, which make use of new deep learning methods to automatically recognize breast images and improve the accuracy of diagnoses made by radiologists. This review is based upon published literature in the past decade (January 2010–January 2020), where we obtained around 250 research articles, and after an eligibility process, 59 articles were presented in more detail. The main findings in the classification process revealed that new DL-CAD methods are useful and effective screening tools for breast cancer, thus reducing the need for manual feature extraction. The breast tumor research community can utilize this survey as a basis for their current and future studies.

1. Introduction

Due to the anatomy of the human body, women are more vulnerable to breast cancer than men. Breast cancer is one of the leading causes of death for women globally [1–4] and is a significant public health problem. It occurs due to the uncontrolled growth of breast cells. These cells usually form tumors that can be seen from the breast area via different imaging modalities.

To understand breast cancer, some basic knowledge about the normal structure of the breast is important. Women's breasts are constructed of lobules, ducts, nipples, and fatty tissues (Figure 1) [5]. Normally, epithelial tumors grow inside the lobes, as well as in the ducts, and later form a lump [6], generating breast cancer.
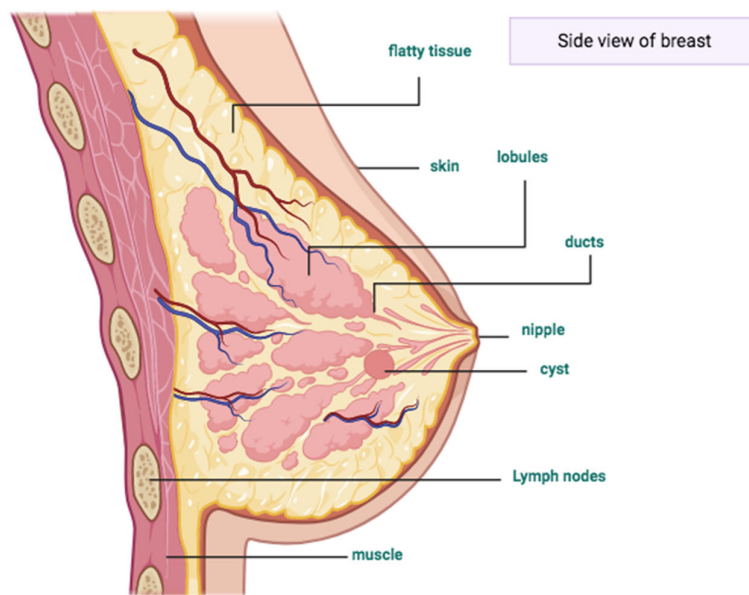
Figure 1. This scheme represents the anatomy of a woman's breast. Inside the lobes are the zones where the epithelial tumors or cyst grow. Designed by Biorender (2020). Retrieved from https://app.biorender.com/biorender-templates

Breast abnormalities that can indicate breast cancer are masses and calcifications [7]. Masses are benign or malignant lumps and can be described in terms of their shape (round, lobular, oval, and irregular) or their margin (obscured, indistinct, and spiculated) characteristics. The spiculated masses are the particular kind of masses that have a high probability of malignancy. A spiculated mass is a lump of tissue with spikes or points on the surface. It is suggestive but not a confirmation of malignancy. It is a common mammography finding in breast carcinoma [8].

On the other hand, microcalcifications are small granular deposits of calcium and may reveal themselves as clusters or patterns (like circles or lines) and appear as bright spots in a mammogram. Benign calcifications are usually larger and coarser with round and smooth contours. Malignant calcifications tend to be numerous, clustered, small, varying in size and shape, angular, and are irregularly shaped [7,9].

Breast cancer screening aims to detect benign or malignant tumors before the symptoms appear, and hence reduce mortality through early intervention [2]. Currently, there are different screening methods, such as mammography [10], magnetic resonance imaging (MRI) [11], ultrasound (US) [12], and computed tomography (CT) [13]. These methods help to visualize hidden diagnostic features. Out of these modalities, ultrasound and mammograms are the most common screening methods for detecting tumors before they become palpable and invasive [2,14–16]. Furthermore, they may be utilized effectively to reduce unnecessary biopsies [17]. These two are the modalities that are reviewed in this article.

A drawback in mammography is that the results depend upon the lesion type, the age of the patient, and the breast density [18–24]. In particular, dense breasts that are "radiographically" hard to see exhibit a low contrast between the cancerous lesions and the background [25,26].

Digital mammography (DM) has some limitations, such as low sensitivity, especially in dense breasts, and therefore other modalities, such as US, are used [12]. US is a non-invasive, non-radioactive, real-time imaging technique that provides high-resolution images [27]. However, all these techniques require manual interpretation by an expert radiologist. Normally, the radiologists try to do a manual interpretation of the medical image via a double mammogram reading to enhance the accuracy of the results [28]. However, this is time-consuming and is highly

prone to mistakes [3,29]. Because of these limitations, different artificial intelligence algorithms are gaining attention due to their excellent performance in image recognition tasks.

Different breast image classification methods have been used to assist doctors in reading and interpreting medical images, such as traditional computer-aided diagnosis/detection (CAD) systems [8,30–32] based on machine learning (ML) [33–35], or based on modern CAD-deep learning (DL) system [36–42].

The goal of CAD is to increase the accuracy and sensitivity rates to support radiologists in their diagnosis decisions [43,44]. Recently, Gao et al. [45] developed a CAD system for screening mammography readings that demonstrated an approximately 92% accuracy in the classification. Likewise, other studies [46,47] used several CNNs for mass detection in mammography's and ultrasounds [48–50].

In general, DL-CAD systems focus on CNNs, which is the most popular model used for intelligent image analysis and for detecting cancer with good performance [51,52]. With CNNs, it is possible to automate the feature extraction process as an internal part of the network, thus minimizing human interference. DL-CAD systems have added broader meaning with this approach, distinguishing it from traditional CAD methods.

The next-generation technologies based on the DL-CAD system solve problems that are hard to solve with traditional CAD [12,33]. These problems include learning from complex data [53-54], image recognition [55], medical diagnosis [56,57], and image enhancement [58]. In using such techniques, the image analysis includes preprocessing, segmentation (selection of a region of interest—ROI), feature extraction/selection, and classification.

In this review, we summarize recent upgrades and improvements in new DL-CAD systems for breast cancer detection/diagnosis using mammograms and ultrasound imaging and then describe the principal findings in the classification process. The following research questions were used as the guidelines for this article:

- How the new DL-CAD systems provide breast imaging classification in comparison with the traditional CAD system?
- Which artificial neural networks implemented in DL-CAD systems give better performance regarding breast tumor classification?
- Which are the main DL-CAD architectures used for breast tumor diagnosis/detection?
- What are the performance metrics used for evaluating DL-CAD systems?

2. Materials and Methods

2.1. Flowchart of the Review

The research process is shown in Figure 2, which was in accordance with the PRISMA (Preferred reporting items for systematic reviews and meta-analyses) flow diagram and protocol [59].

Furthermore, the systematic review process follows the flow diagram and protocol (Figure 3) given in [60].

We identified appropriate studies in PubMed, Medline, Google Scholar, and Web of Science databases, as well as conference proceedings from IEEE (Institute of Electrical and Electronics Engineers), MICCAI (Medical Image Computing and Computer Assisted Intervention), and SPIE (Society of Photographic Instrumentation Engineers), published between January 2010 and January 2020. The search was designed to identify all studies in which DM and US were evaluated as a primary detection modality for breast cancer, and were both used for screening and diagnosis. A comprehensive search strategy including free text and MeSH terms was utilized, including terms such as: "breast cancer," "breast tumor," "breast ultrasound," "breast diagnostic," "diagnostic imaging," "deep learning," "CAD system," "convolutional neural network," "computer-aided detection," "computer-aided diagnoses," "digital databases," "mammography," "mammary ultrasound," "radiology information," and "screening."
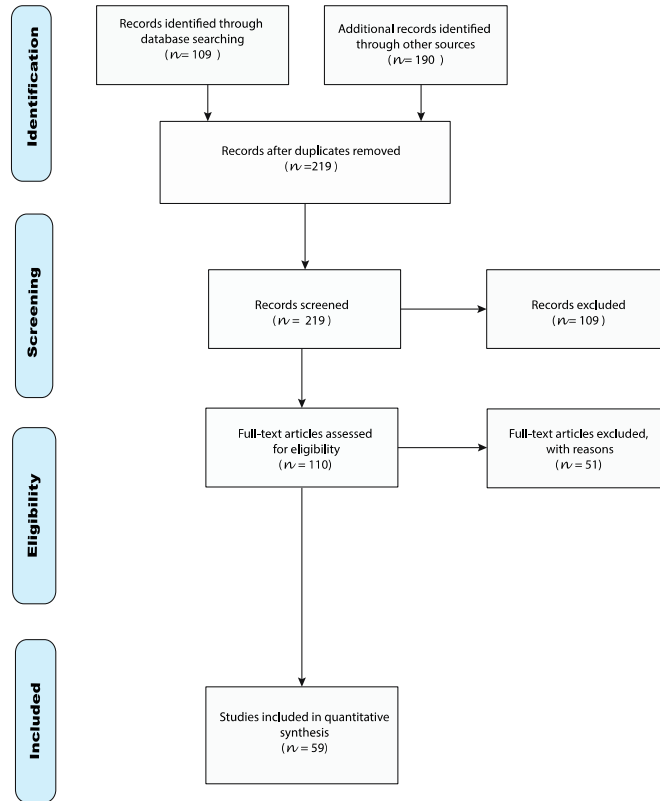
Figure 2. PRISMA flow diagram.
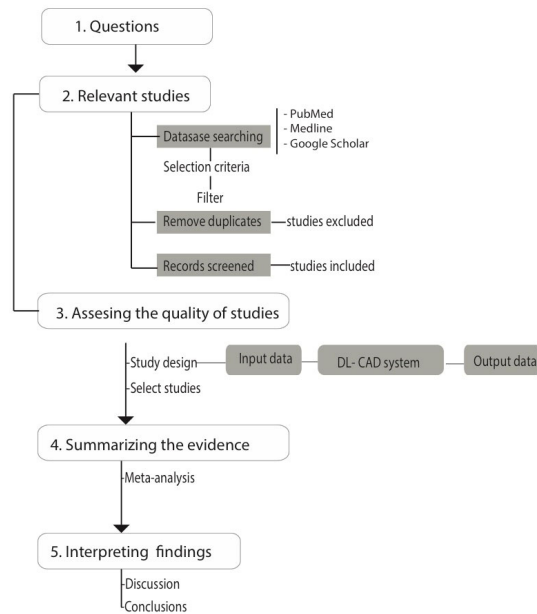
Systematic Review Process

Figure 3. This flowchart diagram represents the review process of articles in this paper. DL-CAD: deep learning computer-aided diagnosis/detection.

2.1.1. Inclusion Criteria

Articles were included if they assessed computer-aided diagnosis (CADx) and/or computer-aided detection (CADe) for breast cancer, DL in breast imaging, deep CNN, DL in mass segmentation and classification in both DM and US, deep neural network architecture, transfer learning, and feature-based methods regarding automated DM breast density measurements. From a review of the abstracts, we manually selected the relevant papers.

2.1.2. Exclusion Criteria

Articles were excluded if the study population included other screening methods, such as MRI, CT, PET (positron emission tomography), or if other machine learning techniques were used.

2.2. Study Design

The general modern DL-CAD design was divided into four sections (Figure 4). First, different mammography and ultrasound public digital databases were analyzed as input data for the DL-CAD system. The second section includes the preprocessing and postprocessing in the next-generation DL-CAD.
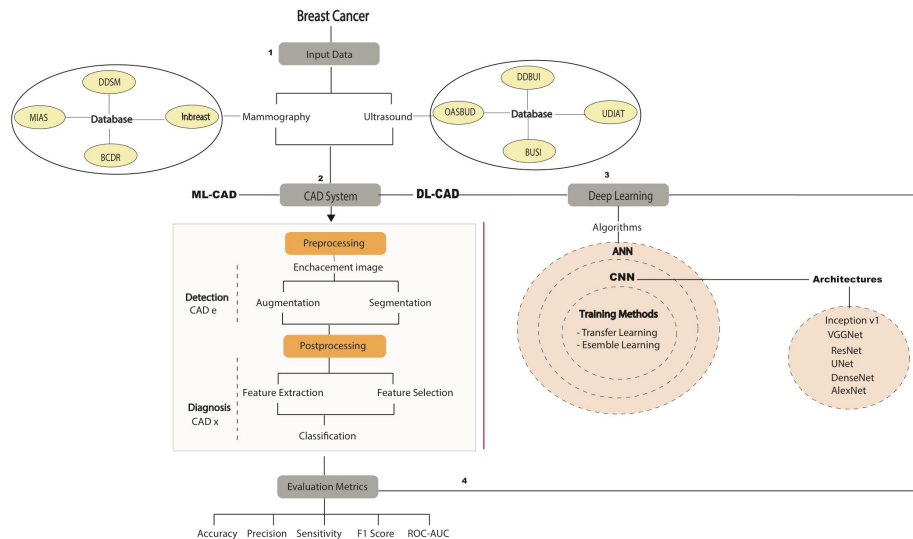
Figure 4. The general diagram is a flowchart that describes how a modern CAD system process can be used with DM and US images from public and private databases. Normally, the CAD system consists of several stages, such as segmentation, feature extraction/selection, and classification. However, DL-CAD systems are based on CNN models and architectures for automatic feature extraction/selection and classification with convolutional and fully connected layers through self-learning. Finally, CAD systems are validated by different metrics. ANN: artificial neural network, BCDR: Breast Cancer Digital Repository, BUSI: Breast Ultrasound Image Dataset, CADe: computer-aided detection, CADx: computer-aided diagnosis, DDBUI: Digital Database for Breast Ultrasound Images, DDSM: Digital Database for Screening Mammography, MIAS: Mammographic Image Analysis Society Digital Mammogram Database, OASBUD: Open Access Series of Breast Ultrasonic Data, ROC–AUC: receiver operating characteristic curve–area under the curve, UDIAT: Ultrasound Diagnostic Ultrasound Centre of the Parc Tauli, VGGNet: Visual Geometry Group.

In the third part, full articles were analyzed to compile the successful CNNs used in DL architectures. Furthermore, the best evaluation metrics were analyzed to measure the accuracy of these algorithms. Finally, a discussion and conclusions about these classifiers are presented.

2.2.1. Public Databases

Normally, DL models are tested using private clinical images or publically available digital databases that are used by researchers in the breast cancer area. The amount of public medical images is increasing because most of the DL-CAD systems require a large amount of data. Thus, DL algorithms are applied to available digitized mammograms, such as those from MIAS (Mammographic Image Analysis Society Digital Mammogram Database) [61], DDSM (Digital Database for Screening Mammography), IRMA (Image Retrieval in Medical Application) [62,63], INbreast [64], and BCDR (Breast Cancer Digital Repository) [45,65], as well as public US databases, such as BUSI (Breast Ultrasound Image Dataset), DDBUI (Digital Database for Breast Ultrasound Images), and OASBUD (Open Access Series of Breast Ultrasonic Data) from the Oncology Institute in Warsaw, Poland, and the private US collected datasets, such as SNUH (Seoul National University Hospital, Korea) [48], Dataset A (collected in 2001 from a professional didactic media file for breast imaging specialists) [66], and Dataset B collected from the UDIAT(Ultrasound Diagnostic Ultrasound Centre of the Parc Tauli) Corporation, Sabadell, Spain. These widely used datasets are listed in Table 1.

Table 1. Summary of the most commonly used public breast cancer databases in the literature.

Type	Database	Annotations	Link	Author
Mammograms	DDSM	2620 patients including mediolateral oblique (MLO) and craniocaudal (CC) images for classification.	http://www.eng.usf.edu/cvprg/Mammography/Database.html	Jiao et al. [67]
	BCDR	736 biopsy prove lesion of 344 patients, including CC and MLO images for classification.	https://bcdr.eu/	Arevalo et al. [68]
	INbreast	419 cases, including CC and MLO images of 115 patients, for detection and diagnosis.	http://medicalresearch.inescporto.pt/breastresearch/index.php/Get_INbreast_Database	IMoreira et al. [64]
	Mini-MIAS	322 digitized MLO images of 161 patients for segmentation, detection, and classification.	http://peipa.essex.ac.uk/info/mias.html	Peng et al. [69]
Ultrasound	BUSI	The dataset consists of 600 female patients. The 780 images include 133 normal images without masses, 437 images with cancer masses, and 210 images with benign masses. This set is utilized for classification, detection, and segmentation.	https://scholar.cu.edu.eg/?q=afahmy/pages/dataset	Dhabyani et al. [70]
	DDBUI	285 cases and 1132 images in total for classification.	https://www.atlantis-press.com/proceedings/jcis2008/1735	Tian et al. [71]
	Dataset A	Private dataset with 306 (60 malignant and 246 benign) images, which are utilized for detection.	goo.gl/SJmoti	Yap et al. [48]
	Dataset B	Private dataset with 163 (53 malignant and 110 benign) images.		Byra et al. [66]
	SNUH	Private dataset with a total of 1225 patients with 1687 tumors. This study includes biopsy diagnosis.		Moon et al. [49]
	OASBUD	52 malignant and 48 benign masses, which are utilized in image processing algorithms.	http://bluebox.ippt.gov.pl/~hpiotrzk	Piotrzkowska et al. [72]
	ImageNet	882 US images (678 benign and 204 malignant lesions), which are utilized in object recognition, image classification, and automatic object clustering.	http://www.image-net.org/	Deng et al. [73]

SNUH: Seoul National University Hospital.

2.2.2. CAD Focused on DM and US

The CAD systems are divided into two categories. One is the traditional CAD system and the other is the DL-CAD system (Figure 5). In the traditional CAD system, the radiologist or clinician defines features in the image, where there can be problems regarding recognizing the shape and density information of the cancerous area. A DL-CAD system, on the other hand, creates such features by itself through the learning process [74].
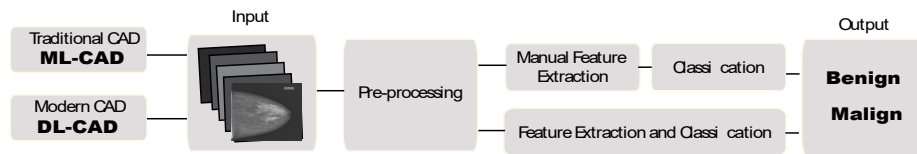
Figure 5. The scheme describes the main difference between the traditional machine learning (ML)-CAD system and the DL-CAD system.

Furthermore, CAD systems can be broken down into two main groups: CADe and CADx. The main difference between CADe and CADx is that the first refers to a software tool that assists in ROI segmentation within an image [75], identifying possible abnormalities and leaving the interpretation to the radiologist [8]. On the other hand, CADx serves as a decision aid for radiologists to characterize findings from a CADe system. Several significant CAD works are described in Table 2.

Table 2. The traditional CAD system summary with DM and US breast cancer images. It covers four stages: (i) image processing, (ii) segmentation, (iii) feature extraction and selection, and (iv) classification.

Reference	Models	Description	Application
[76,77]	Pixel-based, which is based on the curvature of the edge and clustering [3,78]: conventional (CLAHE), region-based, feature-based (wavelet), and fuzzy.	Pectoral removal techniques are not sufficient to provide accurate results. Thereby, intensity-based methods, line detection, statistical techniques, wavelet methods, and the active contour technique have also been tried for segmenting this area. Its accuracy varies from 84% to 99%, where the active contour technique reached the highest value of 99%, followed by the wavelet method with 93% [79]. Enhancement techniques are divided into three categories: spatial, frequency domain, and a mixture of these two. These categories can be classified into four models. The region-based method requires a seed point and it is time-consuming.	Preprocessing
[80,81]	Local thresholding and region-growing [82]; edge detection, template matching [12,83], and a multiscale technique [84];	The thresholding method shows greater stability but is dependent on the parameter selection. Furthermore, is not sufficient for segmenting fatty tissue in a DM because its images contain noise and have low contrast and intensity. The region-growing method is well-known in micro-calcification detection and uses pixel properties for	Segmentation

	NN [85].	segmenting fatty tissue. Edge detection utilizes the wavelet transform in a multiscale structure to represent signals and variations in US images. Template matching requires a comparison with a given image (ROI) with a template image to measure the similarity between both. Finally, an NN utilizes a multi-layered perceptron with a hidden layer for extracting the contours of tumors automatically; nevertheless, training an NN is time-consuming.	
[86]	PCA [87], LDA [88], and GLCM [89].	Feature selection methods: wrapper and filter (chi-square [90]). The most well-known feature extraction techniques are PCA, LDA, GLCM, gain ratio, recursive feature [91], RF, WPT [92,93], Fourier power spectrum [94], Gaussian [95] and DBT [29]. PCA feature extraction techniques are better at reducing the high-dimensional correlated features into low dimensional features [87].	Feature Selection and extraction
[12,33]	SVM [96,97] and ANN [98,99].	SVM is useful in DM classification because these are highly overlapping and nonlinear in their feature space. It minimizes the generalization error during the process of testing data and is much more accurate and computational efficient because of the reduced number of parameters. ANN: Backpropagation, SOM, and hierarchical ANN. The performance of back-propagation is better than that of linear classifiers. However, the training process is stochastic and unrepeatable, even with the same data and initial conditions. Prone to overfitting due to the complexity of the model structure. Finally, advantages and disadvantages from other classifiers have been previously discussed in several studies: KNN [100], BDT [101], simple logistic classifier [102], and DBN [103]	Classification

2.2.3. Preprocessing

It is known that the database characteristics can significantly affect the performance of a CAD scheme, or even a particular processing technique. Furthermore, it can develop a scheme that yields erroneous or confusing results [104] since radiological images contain noise, artefacts, and other factors that can affect medical and computer interpretations. Thus, the first step in preprocessing is to improve the image quality, contrast, removal noise, and pectoral muscle [105].

Image Enhancement

The main purpose of image preprocessing is to enhance the image and suppress noise while preserving important diagnostic features [106,107]. Preprocessing for breast cancer diagnosis also

consists of delineation of the tumors from the background, breast border extraction, and pectoral muscle removal. The pectoral muscle segmentation is a challenge in mammogram image analysis because the density and texture information is similar to that of the breast tissues. Furthermore, it depends on the standard view used during mammography. Generally, mediolateral oblique (MLO) and craniocaudal (CC) views are used [78].

As noted, DM includes many sources of noise, which are classified as a high-intensity, low-intensity, or tape artefacts. The principal noise models observed in mammography are salt and pepper, Gaussian, speckle, and Poisson noise.

In the same way, US images suffer from noise, such as intensity inhomogeneity, a low signal-to-noise ratio, high speckle noise [108,109], blurry boundaries, shadow, attenuation, speckle interference, and low contrast. Speckle noise reduction techniques are categorized in filtering, wavelet, and compound methods [12].

Thus, many traditional filters can be applied for noise removal, including a wavelet transform, median filter, mean filter, adaptive median filter, Gaussian filter, and adaptive Wiener filter [3,110–113]. Furthermore, different traditional methods, such as histogram equalization (HE) [114,115], adaptive histogram equalization (AHE) [116], and contrast-limited adaptive histogram equalization (CLAHE) [117], can be used to enhance the image.

On the other hand, deep CNNs [118] are gaining attention for improving super-resolution [119] images (SR) based on a CNN, namely, (i) multi-image super-resolution and (ii) single-image super-resolution [120,121]. Among the most used algorithms for generating high-resolution (HR) imaging [122,123] are nearest-neighbor interpolation [124], bilinear interpolation [125], and bicubic interpolation [126].

Image Augmentation

Deep CNN depends on large datasets to avoid overfitting and is necessary for good DL model performance [127]. Thus, limited datasets are a major challenge in medical image processing [128] and it is necessary to implement data augmentation techniques. There are two common techniques for increasing the data in DL, namely, data augmentation and transfer learning/fine-tuning [129,130]. Examples of DL models that have been trained with data augmentation are Imagenet [74] and transfer learning [47].

The image augmentation algorithms include basic image manipulations (flipping, rotation, transformation, feature space augmentation, kernel, mixing images, and random erasing [131]) and DL manipulations (generative adversarial networks (GANs)) [132], along with a neural style transfer [133] and meta-learning [128]). These techniques increase the amount of data by preprocessing input image data via operations such as contrast enhancement and noise addition, which have been implemented in many studies [134–140].

Image Segmentation

This processing step plays an important role in image classification. Segmentation is the separation of ROIs (lesions, masses, and microcalcifications) from the background of the image.

In traditional CAD systems, the tasks of specifying the ROI, such as an initial boundary or lesions, are accomplished with the expertise of radiologists. The traditional segmentation task in DM can be divided into four main classes: (i) threshold-based segmentation, (ii) region-based segmentation, (iii) pixel-based segmentation, and (iv) model-based segmentation [3,78]. Furthermore, US image segmentation includes several techniques: threshold-based, region-based, edge-based, water-based, active-contour-based, and neural-network-learning-based techniques [141,142].

The accuracy of the segmentation affects the results of CAD systems because numerous features are used for distinguishing malignant and benign tumors (texture, contour, and shape of lesions). Thus, the features may only be effectively extracted if the segmentation of tumors is performed with great accuracy [106,142]. This is why researchers are using DL methods, especially CNNs, because these methods have shown excellent results on segmentation tasks. Furthermore, DL-CAD systems

are independent of human involvement and are capable of autonomously modeling breast US and DM knowledge using constraints. Two strategies have been utilized for full image sizes for training CNNs for DM and US instead of ROIs: (1) high-resolution [143] and (2) patch-level [144] images. For example, recent network architectures that have been used to produce segmented regions are YOLO [145], SegNet [146,147], UNet [148], GAN [149], and ERFNet [150].

2.2.4. Postprocessing

Image Feature Extraction and Selection

After the segmentation, feature extraction and selection are the next steps to remove the irrelevant and redundant information of the data being processed. Features are characteristics of the ROI taken from the shape and margin of lesions, masses, and calcifications. These features can be categorized into texture and morphologic features [12,86], descriptors, and model-based features [52], which help to discriminate between benign and malignant lesions. Most of the texture features are calculated from the entire image or ROIs using the gray-level value and the morphological features.

There are some traditional techniques used for feature selection, such as searching algorithms, the chi-square test, random forest, gain ratio, and recursive feature elimination [91]. In addition, other traditional techniques used for the feature extraction include principal component analysis (PCA), wavelet packet transform (WPT) [92,93], grey-level co-occurrence matrix (GLCM) [91], Fourier power spectrum (FPS) [94], Gaussian derivative kernels [95], and decision boundary features (DBT) [151].

However, in some classification processes, such as an ANN or support vector machine (SVM), the dimension of the vectors affects both the computational time and the performance [152] because this depends on the number of features extracted. Thus, feature selection techniques reduce the size of the feature space, improving the accuracy and computation time by eliminating redundant features [153]. In particular, DL models produce a set of image features from the data [154], whose main advantage is that they extract features and perform classifications directly. Providing good extraction and selection of the features is a crucial task for DL-CAD systems; for example, some CNNs that are capable of extracting features have been presented by different authors [155,156].

2.2.5. Classification

During the classification process, the dimension of feature vectors is important because these affect the performance of the classifier. The features of breast US images can be divided into four types: texture, morphological, model-based, and descriptor features [86]. After the features have been extracted and selected, they are input into a classifier to categorize the ROI into malignant and benign classes. The commonly used classifiers include linear, ANN, Bayesian neural networks, decision tree, SVM, template matching [106], and CNNs.

Recently, deep CNNs, which are hierarchical architectures trained on large-scale datasets, have shown stunning performances regarding object recognition and detection [157], which suggests that these could also improve breast lesion detection in both US and DM methods. Some researchers are interested in lesion [158], microcalcification [159,160], and mass [161,162] classification in DM and US [15–154,163–165] images based on CNN models.

Deep Learning Models

DL in medical imaging is mostly represented by a basic structure called a CNN [57,75]. There are different DL techniques, such as GANs, deep autoencoders (DANs), restricted Boltzmann machine (RBM), stacked autoencoders (SAEs), convolutional autoencoders (CAEs), recurrent neural networks (RNNs), long short-term memory (LSTM), multiscale convolutional neural network (M-CNN), and multi-instance learning convolutional neural network (MIL-CNN) [3]. DL techniques have been implemented to train neural networks for breast lesion detection, including ensemble [75] and transfer learning [129,157,166] methods. The ensemble method combines several basic models in

order to get an optimal model [167], and transfer learning is an effective DL method to pre-train models to deal with small datasets, as in the case of medical images.

ANNs are composed of an input and output layer, plus one or more hidden layers, as shown in Figure 6. In the field of breast cancer, three types of ANN are frequently used: backpropagation, SOM, and hierarchical ANNs. To train an ANN with a backpropagation algorithm, the error function is given to calculate the gradient descent. This error propagates in the backward direction and the weights are adjusted for error reduction. This processing is repeated until the error becomes zero or a minimum [2].
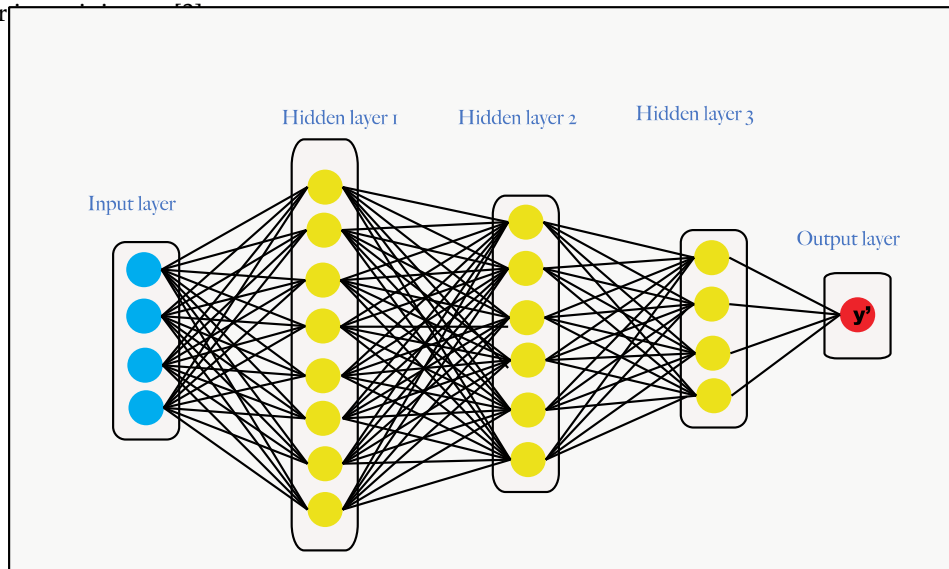
Figure 6. An ANN learns by processing images, where each of which contains an input, hidden, and result layer.

Convolutional Neural Networks

CNNs are the most widely used Neural Networks when it comes to DL and medical image analysis. The CNN structure has three types of layers: (i) convolution, (ii) pooling, and (iii) full-connection layers, which are stacked in multiple layers [74]. Thus, a CNN's structure is determined by different parameters, such as the number of hidden layers, the learning rate, the activation function (rectified linear unit (ReLU)), pooling layer for feature map extraction, loss function (softmax), and the fully connected layers for classification, as shown in Figure 7.
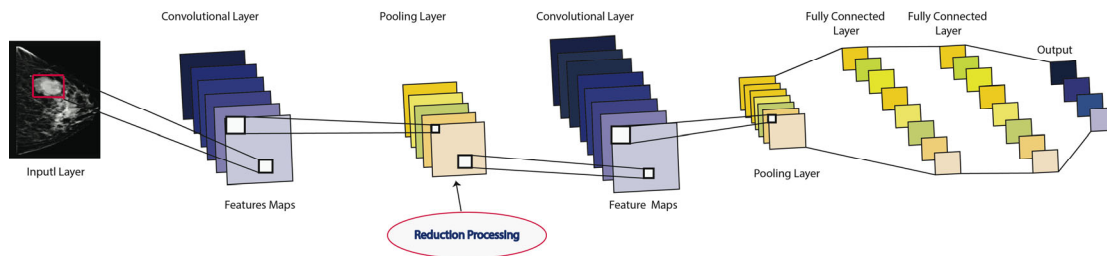
Figure 7. A feed-forward CNN network, where the convolutional layers are the main components, followed by a nonlinear layer (rectified linear unit (ReLU)), pooling layer for feature map extraction, loss function (softmax), and the fully connected layers for classification. The output can be either benign or malignant classes.

Furthermore, there are several methods for improving a CNN's performance, such as dropout and batch normalization. Dropout is a regularization method that is used to prevent a CNN model

from overfitting. A batch normalization layer speeds up the training of CNNs and reduces the sensitivity to network initialization.

2.2.6. Evaluation Metrics

Different quantitative metrics are used to evaluate the classifier performance of a DL-CAD system. These include accuracy (Acc), Sensitivity (Sen), Specificity (Spe), area under the curve (AUC), F1 score, and a confusion matrix. The statistical equations are shown in Tables 3 and 4.

Table 3. Confusion matrix for a binary classifier that is used to distinguish between two classes, namely, benign and malignant. TP: true positive; FN: false negative, FP: false positive, TN: true negative, TPR: true positive rate, FPR: false positive rate.

Classes	Predicted Classes		Equation
	C_1	C_2	
C_1 (Benign)	TP	FN	$TPR = \left(\dfrac{TP}{TP + FN} \right)$
C_2 (Malignant)	FP	TN	$FPR = \left(\dfrac{FP}{FP + TN} \right)$

Table 4. Validation assessment measures.

Model	Equation
Accuracy	$Acc = \left(\dfrac{TP + TN}{TP + TN + FP + FN} \right)$
Sensitivity	TPR
Specificity	$TNR = \left(\dfrac{TN}{TN + FN} \right)$
Precision	$Precision = \left(\dfrac{TP}{TP + FP} \right)$
F1 Score	$F1\ score = 2x \left(\dfrac{precision \times recall}{precision + recall} \right)$
MCC	$MCC = \dfrac{TP \times TN - FP \times FN}{\sqrt{(TP + FP)(TP + FN)(TN + FP)(TN + FN)}}$

The receiver operating characteristic curve (ROC) is a graph for plotting the true positive rate (TPR) versus a false positive rate (FPR) and is derived from the AUC. The TPR and the FPR are also called sensitivity (recall) and specificity, respectively, as shown in Figure 8.
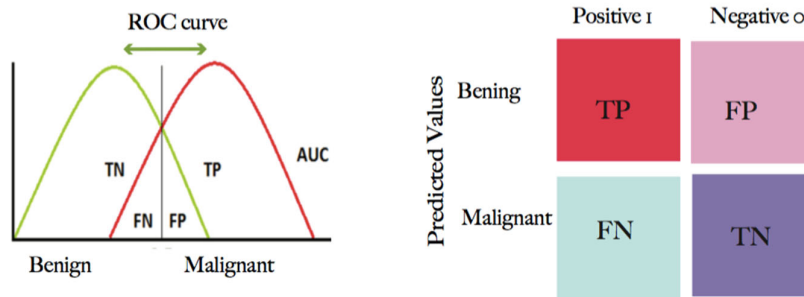
Figure 8. The confusion matrix for the ROC. The number of images correctly predicted by the classifier is located on the diagonal. The ROC curve utilizes the TPR on the *y*-axis and the FPR on the *x*-axis.

The AUC provides the area under the ROC curve and a perfect score has a range from 0.5 to 1. A 100% correct classified version will have an AUC value of 1 and it will be 0 if there is a 100% wrong classification [168].

Cross-validation is a statistical technique that is used to evaluate predictive models by partitioning the original samples into training, validation, and testing sets. There are three types of validation: (1) hold-out splits (training 80% and testing 20%), (2) three-way data split (training 60%, validation 20%, and testing 20%), and (3) K-fold cross-validation (from 3 to 5 k-fold for a large data set, 10 k-fold for a small dataset), where the data are split into k different subsets depending on their size [65].

3. Results

3.1. CNN Architectures

A model's performance depends on the architecture and the size of the data. In this sense, there are different CNN architectures that have been proposed: AlexNet [169], VGG-16 [170], ResNet [171], Inception (GoogleNet) [172], and DenseNet [173]. These networks have shown promising performance in recent works for image detection and classification. Table 5 shows a brief description of these networks.

Table 5. Summary of CNN architecture information for breast imaging processing.

Reference	Model	Description	Training Method	Application
Krizhevsky et al. [169]	AlexNet	A deep CNN evaluated using the Imagenet [65] LSVRC-2010 dataset [173], with top-1 and top-5 error rates of 37.5% and 17.0%, respectively. This achieved a top-5 test error rate of 15.3% compared to 26.2% (ImageNet Large-Scale Visual Recognition Challenge (ILSVRC) 2012).	Dropout model	Classification
Samala et al. [174]	DL-CNN	CAD system for masses in DBT volume, which is trained using transfer learning. The best AUC obtained was 0.933 and the improvement was statistically significant ($p < 0.05$).	CNN architecture	Detection tomosynthesis from DM
Simoyan et al. [170]	VGG-VD	The very deep (VD)-CNN models (VGG-VD16 and VGG-VD19 [158]) were evaluated in ILSVRC 2014 (ImageNet).	Deep ConvNet architecture	Classification
He et al. [171]	ResNet	An ensemble of these residual nets achieved a 3.57% error on the ImageNet (ILSVRC 2015) test set.	ResNet with a depth of up to 152 layers 8× deeper	Classification
Huang et al. [172]	DenseNet	DenseNet was proposed to reduce the vanishing gradient problem, to reduce the number of parameters, and to strengthen the feature propagation.	ImageNet with a CNN	Object recognition
Szegedy et al. [27]	Inception v5	A deep CNN was evaluated in ILSVRC 2014.	Deep-CNN	Classification and detection
Das et al. [175]	VGGNet	BreakHist dataset with 58 malignant and 24 benign cases was evaluated with a deep CNN. The best accuracy percentage was reached with 100× (89.06%).	MIL architecture	Histopathology
Cao et al. [152]	Deep CNN	Private dataset that contains 577 benign and 464 malignant cases.	Detection: Fast R-CNN, Faster R-CNN, YOLOv3, and SSD; Classification: AlexNet, VGG, ResNet, GoogleNet, ZFNet, and Densenet	US lesion detection and classification
Chiao et al. [153]	Deep CNN	Private US imaging dataset that contains 307 images with 107 benign and 129 malignant cases.	Mask R-CNN with ROI alignment;	Sonogram lesion detection and

			based on a faster R-CNN using an RPN to extract features	classification
Yap et al. [48]	LeNet, UNet, deep CNN	This work studies the performance of CNNs in breast US detection using two private datasets A and B.	LeNet [163], U-Net [148], and transfer learning [176]	US breast lesion detection
Geras, K. et al. [176]	Multi-view DL-CNN	INbreast [77] and DDSM [58] databases were used; the model achieved an AUC of 0.68%.	The CNN is jointly trained using stochastic gradient descent with backpropagation [175,176] and data augmentation via random cropping [168,177]	High-resolution, augmentation, and DM classification
Han et al. [62]	GoogleNet with ensemble learning	Dataset contains a total of 7408 US breast images, with 657 used as the training set and 829 as the test set. The accuracy reached was 90.21%.	The CNN was trained with 10-fold cross-validation. Data augmentation was carrying out with the Caffe method	Data augmentation, detection, and classification of breast lesions in US
Dhungel et al. [178]	LeNet for CNN models in cascade R-CNN	INbreast dataset was used, with 115 cases and 410 images from MLO and CC views. The results showed that the DL-CAD system is able to detect 90% of masses, with a segmentation accuracy of 85% and the classification reached a sensitivity of 0.98 and a specificity of 0.7.	DL detection: Fast R-CNN, multiscale-DBN, and random forest; DL segmentation: CRF; DL classification: regression method.	Detection, segmentation, and classification of masses in DM
Singh et al [165]	GAN	The Mendeley database [179] was used, which contains 150 malignant and 100 benign tumors. The performance metrics achieved scores of dice = 93.76% and IoU = 88.82%.	Segmentation with GAN learning.	Segmentation and classification of US images
Cheng, J. Z. [37]	SDAE based CADx	The method was carried out on a private database, with 520 breast sonograms (275 benign and 245 malignant lesions). The AUC performance reached 0.80%.	An SDAE (OverFeat) model was used to classify with the ensemble method.	Breast lesion/nodules diagnosis and classification of US images

3.2. Performance Metrics

Furthermore, brief reviews of the DL architectures based on DM and US breast images, along with their evaluation metrics, are presented in Tables 6 and 7 [50,180].

Table 6. The quantitative indicators that were used to evaluate the performance between different CNN architectures in DM datasets.

Reference	Database	Deep CNN Model	Acc (%)	Sen (%)	Spec (%)	Precision (%)	F1 Score (%)	AUC (%)
Al-Masni et al. [145]	DDSM with 600 DM.	CNN YOLO5: Fold cross-validation in both datasets; mass classification	99	93.20	78	-	-	87.74
	DDSM augmentation with 2.400	Mass detection	97	100	94	-	-	96.45
Ragab et al. [168]	DDSM with 2620 cases	Deep-CNN-based linear SVM using ROI manually	79	76.3	82.2	85	80	88
	CBIS-DDSM with 1644 cases	ROI threshold	80.5	77.4	84.2	86	81.5	88
		SVM-based medium Gaussian	87.2	86.2	87.7	88	87.1	94
Duggento et al. [180]	CBIS-DDSM	Deep CNN	71	84.4	62.4	-	-	77
Chougrad et al. [181]	BCDR	Inceptionv3	96.67	-	-	-	-	96
	DDSM		97.35	-	-	-	-	98
	INbreast		95.50	-	-	-	-	97
	MIAS		98.23	-	-	--	-	99

Table 7. The quantitative indicators that were used to evaluate different CNN architectures' performances on US datasets.

Reference	Database	Deep CNN Model	Acc (%)	Sen (%)	Spec (%)	Precision (%)	F1 Score (%)	AUC (%)
Moon et al. [49]	BUSI SNUH	VGGNet-like	84.57	73.65	93.12	89.34	80.74	91.98
		VGGNet 16	84.57	73.64	93.12	89.34	80.74	93.22
		ResNet 18	81.60	86.49	77.77	75.29	80.50	91.85
		ResNet 50	81.60	75.68	86.24	81.16	78.32	88.83
		ResNet 101	84.57	75,00	92.06	88.10	81.02	91.04
		DenseNet 40	85.46	79.05	90.48	86.67	82.69	93.52
		DenseNet 12	86.35	77.70	93.12	89.84	83.33	92.48
		DenseNet 161	83.09	69.59	93.65	89.57	78.33	89.18
Byra et al. [66,182]	ImageNet	VGG19	88.7	0.848	0.897	-	-	93.6
	UDIAT		84	0.851	0.834	-	-	89.3
	OASBUD [150]		83	0.807	0.854	-	-	88.1
Cao et al. [152]	Private dataset consisting of 579 benign and 464 malignant cases	Single Shot Detector (SSD)300 + ZFNet	96.89	67.23	-	-	79.38	-
		YOLO	96.81	65.83	-	-	78.37	-
		SSD300 + VGG16	96.42	66.70	-	-	78.85	-
Han et al. [62]	Private database with a total of 7408 US images with 4254 benign and 3154 malignant lesions	CNN-based GoogleNet	91.23	84.29	96.07		-	91
Shan et al. [35]	Private database containing 283 breast US images (133 cases are benign and 150 cases are malignant)	ANN	78.1	78	78.2	-	-	82.3

Furthermore, Table 8 gives a brief overview of the new DL-CAD systems' approaches and the traditional ML-CAD systems.

Table 8. DL-CAD systems vs. traditional ML-CAD systems.

Reference	Application	Method	Dataset	Acc (%)	Sen (%)	Spec (%)	AUC (%)	Error (%)
Dheeba [183]	DM classification	ML wavelet neural network	Private database consisting of 216 multiview CC and MLO images.	93.67	94.16	92.10	96.85	96.85
Trivizakis et al. [184]	DM classification	ML with transfer learning and features based on ImageNet and CNN architecture	Mini MIAS and DDSM	79.3	-	-	84.2	-
				74.8	-	-	78.00	-
Samala et al. [185]	DM classification	Multitask transfer learning by a Deep CNN	ImageNet	90	-	-	82	-
Jadoon et al. [186]	DM extraction and classification	CNN + wavelet	IRMA, DDSM, and MIAS	81.83	-	-	83.1	15.43
		CNN + SVM		83.74	-	-	83.9	17.46
Debelee et al. [42]	DM extraction	CNN + SVM	MIAS	97.46	96.26	100	-	-
			DDSM	99	99.48	98.16	-	-
			MIAS	87.64	96.65	75.73	-	-
		MLP	DDSM	97	97.40	96.26	-	-
			MIAS	91.11	86.66	100	-	-
		KNN + SVM	DDSM	97.18	100	95.65	-	-
Ahmed et al. [187]	DM detection	Deep CNN with five–fold cross-validation	INbreast	80.10	80	-	78	-
Xu et al. [51]	US image segmentation	Deep CNN	Private 3D breast US	90.13	88.88	-	-	-
Shan et al. [35]	US image segmentation	ML decision tree	Private breast US consisting of 283 images, where 133 cases are benign and 150 cases are malignant	77.7	74.0	82.0	80	-
		ANN		78.1	78.0	78.2	82	-
		Random forest		78.5	75.3	82	82	-
		SVM		77.7	77.3	78.2	84	-
Gu et al. [188]	3D US image segmentation	Preprocessing: morphological reconstruction; segmentation: region-based approach	Private database with 21 cases, with masses prior to biopsy	85.7	-	-	-	-
Zhang et al. [36]	US image feature extraction and classification	DL architecture	The private dataset consisting of 227 elastography images, with 135 benign tumors and 92 malignant tumors	93.4	88.6	97.1	94.7	-
Almajalid et al. [147]	US image segmentation	DL-CNN architecture U-net	The private dataset containing 221 BUS images	82.52	78.66	18.59	-	-
Singh et al. [189]	US image classification	ML fuzzy c-means and backpropagation ANN	178 breast US containing 88 benign and 90 malignant cases	95.86	95.14	96.58	95.85	-
Cheng et al. [37]	US (sonogram) classification	DL-SDAE	520 breast US (275 benign and 245 malignant lesions)	82.4	78.7	85.7	89.6	_
Shi, et al. [190]	US image classification	Deep polynomial network	A total of 200 pathology-proven breast US images	92.40	92.67	91.36	-	-

4. Discussion and Conclusions

Considering that breast tumor screening using DM has some consequences and limitations because a higher number of unnecessary biopsies and ionizing radiation exposure endangers the patient's health [12], along with low specificity and high FP results, which imply higher, recall rates and higher FN results [191]. This is why US is used as the second choice for DM. Thus, US imaging is one of the most effective tools in breast cancer detection because it has been shown to achieve high accuracy in mass detection, classification [38], and diagnosis of abnormalities in dense breasts [192].

For the abovementioned reasons, we have addressed using both kinds (DM and US) of images in this review, focusing on different ML and DL architectures applied in breast tumor processing, and offering a general overview of databases and CNNs, including their relation and efficacy in performing segmentation, feature extraction, selection, and classification tasks [192].

Thus, according to the research shown in Table 1, the most utilized databases for DM images are MIAS and DDSM, and for US image classification, the public databases BUSI, DDBUI, and OASBUD are most used. The DM images contributed to 110 and 168 published conference papers for the DDSM and MIAS databases, respectively [5]. However, the databases report some limitations and advantages; for example, the MIAS database contains a limited number of images, strong noise, and low-resolution images. In contrast, the DDSM contains a big dataset. Likewise, INbreast contains high-resolution images but has a small data size. BCDR, in comparison with DDSM, has been used in a few studies. Some details about the others strengths and limitations of these databases are discussed in Abdelhafiz [65].

Thereby, Table 2 shows a summary of traditional ML-CAD systems that use public and private databases of DM and US breast images. It covers (i) image preprocessing and (ii) postprocessing steps. This is in contrast with Table 5, which shows a brief summary of DL-CAD systems based on CNN architectures in both types of digital breast images. Thus, in Table 5, various DL architectures and their training strategies for detection and classification tasks are discussed. Based on the most popular datasets, CNN seems to perform rather well, as demonstrated by Chiao et al., Yap et al., and Samala et al. [48,153,174]. Furthermore, [169,173] used several preprocessing and postprocessing techniques for high-resolution [58] data augmentation, segmentation, and classification. The most commonly CNNs used are AlexNet, VGG, ResNet, DenseNet, Inception (GoogleNet), LeNet, and UNet, which employ recent Python libraries for implementing CNNs, such as Tensorflow, Caffe, and Keras, with different hyper-parameters to training the network [55].

Most of these DL architectures use a large data set; thus, it is required to apply an augmentation technique to avoid overfitting and to have better performance during classification. In this sense, the researchers mentioned in Tables 6 [145,168,180,181] and 7 [35,49,62,66,152,182] the authors used transfer learning and ensemble methods, such as data augmentation, to improve the performance of the CNN network, reaching an 89.86% accuracy and 0.9578% AUC in DM, and an AUC of 0.68% on US images. Furthermore, Singh et al. [165] showed that the results obtained with a GAN for breast tumor segmentation outperformed the UNet model, and the SegNet and ERFNet models yielded the worst segmentation results on US images.

In addition, according to Cheng et al. [37], DL techniques could potentially change the design paradigm of CADx systems due to their several advantages over the traditional CAD systems. These are as follows: First, DL can directly extract features from the training data. Second, the feature selection process will be significantly simplified. Third, the three steps of feature extraction, selection, and classification can be realized within the same deep architecture. Thus, SDAE architecture can potentially address the issues of high variation in either the shape or appearance of lesions/tumors. Furthermore, various studies [41,39,40,55] prove that those CNN methods that compare images from CC and MLO views improve the accuracy of detection and reduce the FPR.

Furthermore, different evaluation metrics are described in Tables 3 and 4 as corroboration of the performance of these techniques. The results in Tables 6 and 7 describe different research where their authors have used a variety of datasets (Table 1), approaches, and performance metrics to evaluate CNN techniques in DM and US imaging. For example, better results were achieved in DM analysis by Al-Masni [145] with YOLO5 using DDSM data augmentation, while Chougrad et al. [181] used a deep CNN (Inception V3) with DDSM and MIAS datasets. On the other hand, Moon et al. [49] introduced a DenseNet model to analyze private (BUSI and SNUH) US datasets. Byra et al. [66] achieved high accuracy with the VGG19 deep CNN model using the ImageNet database. Similarly, Cao et al. [152] attained an accuracy of 96.89% with SSD + ZFNet and Han et al. [62] reached 91.23% using a private dataset with GoogleNet.

Likewise, Table 8 contains a literature review for the comparison of the evaluation metrics between DL-CAD systems and traditional ML-CAD systems. Even though Table 8 shows that

Deheeba et al. [183] presented a good traditional wavelet neural network CAD system with high accuracy (93.67%) and AUC of 96.85%, Debelee et al. [42] exceeded this percentage using a CNN + SVM DL-CAD system with DDSM (99%) and MIAS (97.18%) DM datasets. In US images Zhang et al. [36] and Shi et al. [190] proved that a DL-CAD based on CNN and a deep polynomial network achieved better results in terms of accuracy (93.4 and 92.40%) and AUC (94.7%), respectively. In the same way, DL-CAD reached higher values than ML-CAD when used on private US images. For example, Shan et al. [35] and Singh et al. [41] showed ML based on an ANN for segmentation and classification that reached accuracies of 78.5 and 95.86% and an AUC of 82%, respectively. These works demonstrate that in most cases, the DL architectures outperformed traditional methodologies.

To conclude, the use of DL could be a promising new technique to obtain the main features for automatic breast tumor classification, especially in dense breasts. Furthermore, in medical image analysis, using DL has proven to be better for researchers compared to a conventional ML approach [41,42]. It appears as though DL provides a mechanism to extract features automatically through a self-learning network, thus boosting the classification accuracy. However, there is a continuing need for better architectures, more extensive datasets that overcome class imbalance problems, and better optimization methods.

Finally, the main limitation in this work is that several algorithms and results are not available in the open literature because of proprietary intellectual property issues.

Author Contributions: Conceptualization, Y.J.-G. and V.L.; methodology, Y.J.-G.; formal analysis, Y.J.-G., M.J.R.-Á., and V.L.; investigation, Y.J.-G.; resources, Y.J.-G.; writing—original draft preparation, Y.J.-G.; writing—review and editing, Y.J.-G., M.J.R.-Á., and V.L.; visualization, Y.J.-G.; supervision, M.J.R.-Á. and V.L.; project administration, M.J.R.-Á. and V.L.; funding acquisition, V.L. All authors have read and agreed to the published version of the manuscript.

Conflicts of Interest: The authors declare no conflict of interest.

Abbreviations

ANN	artificial neural network
CADx	computer-aided diagnosis
CADe	computer-aided detection
CNN	convolutional neural network
DM	digital mammography
DL	deep learning
DNN	deep neural network
DL-CAD	deep learning CAD system
CC	craniocaudal
MC	microcalcifications
ML	machine learning
MLO	mediolateral oblique
ROI	region of interest
US	ultrasound
MLP	Muli-layer perceptron
DBT	digital breast tomosynthesis
MIL	multiple instances learning
CRF	conditional random forest
RPN	region proposal network
GAN	generative adversarial network
IoU	intersection over union
SDAE	stacked denoising auto-encoder
CBIS	Curated Breast Imaging Subset

YOLO	You Only Look Once
ERFNet	Efficient Residual Factorized Network
CLAHE	contrast-limited adaptive histogram equalization
PCA	principal component analysis
LDA	linear discriminant analysis
GLCM	grey-level co-occurrence matrix
RF	random forest
DBT	decision boundary features
SVM	support vector machine
NN	neural network
SOM	self-organizing map
KNN	K-nearest neighbor
BDT	binary decision tree
DBN	deep belief networks
WPT	wavelet packet transform

References

1. Bray, F.; Ferlay, J.; Soerjomataram, I.; Siegel, R.L.; Torre, L.A.; Jemal, A. Global cancer statistics. *CA Cancer J. Clin.* **2011**, *68*, 394–424, doi:10.3322/caac.20107.

2. Gao, F.; Chia, K.-S.; Ng, F.-C.; Ng, E.-H.; Machin, D. Interval cancers following breast cancer screening in Singaporean women. *Int. J. Cancer* **2002**, *101*, 475–479, doi:10.1002/ijc.10636.

3. Munir, K.; Elahi, H.; Ayub, A.; Frezza, F.; Rizzi, A. Cancer Diagnosis Using Deep Learning: A Bibliographic Review. *Cancers* **2019**, *11*, 1235, doi:10.3390/cancers11091235.

4. American Cancer Society. *Breast Cancer Facts and Figures 2019*; American Cancer Society: Atlanta, GA, USA, 2019.

5. Nahid, A.-A.; Kong, Y. Involvement of Machine Learning for Breast Cancer Image Classification: A Survey. *Comput. Math. Methods Med.* **2017**, *2017*, 1–29, doi:10.1155/2017/3781951.

6. Skandalakis, J.E. Embryology and anatomy of the breast. In *Breast Augmentation*; Springer: Berlin/Heidelberg, Germany, 2009; pp. 3–24.

7. Dheeba, J.; Singh, N.A. Computer aided intelligent breast cancer detection: Second opinion for radiologists—A prospective study. In *Computational Intelligence Applications in Modeling and Control*; Springer: Cham, Switzerland, 2015; pp. 397–430.

8. Ramadan, S.Z. Methods Used in Computer-Aided Diagnosis for Breast Cancer Detection Using Mammograms: A Review. *J. Health Eng.* **2020**, *2020*, 1–21, doi:10.1155/2020/9162464.

9. Chan, H.-P.; Doi, K.; Vybrony, C.J.; Schmidt, R.A.; Metz, C.E.; Lam, K.L.; Ogura, T.; Wu, Y.; MacMahon, H. Improvement in Radiologists?? Detection of Clustered Microcalcifications on Mammograms. *Investig. Radiol.* **1990**, *25*, 1102–1110, doi:10.1097/00004424-199010000-00006.

10. Olsen, O.; Gøtzsche, P.C. Cochrane review on screening for breast cancer with mammography. *Lancet* **2001**, *358*, 1340–1342, doi:10.1016/s0140-6736(01)06449-2.

11. Mann, R.M.; Kuhl, C.K.; Kinkel, K.; Boetes, C. Breast MRI: guidelines from the European Society of Breast Imaging. *Eur. Radiol.* **2008**, *18*, 1307–1318, doi:10.1007/s00330-008-0863-7.

12. Jalalian, A.; Mashohor, S.B.; Mahmud, H.R.; Saripan, M.I.B.; Ramli, A.R.B.; Karasfi, B. Computer-aided detection/diagnosis of breast cancer in mammography and ultrasound: a review. *Clin. Imaging* **2013**, *37*, 420–426, doi:10.1016/j.clinimag.2012.09.024.

13. Sarno, A.; Mettivier, G.; Russo, P. Dedicated breast computed tomography: Basic aspects. *Med. Phys.* **2015**, *42*, 2786–2804, doi:10.1118/1.4919441.

14. Njor, S.; Nyström, L.; Moss, S.; Paci, E.; Broeders, M.; Segnan, N.; Lynge, E. Breast Cancer Mortality in Mammographic Screening in Europe: A Review of Incidence-Based Mortality Studies. *J. Med. Screen.* **2012**, *19*, 33–41, doi:10.1258/jms.2012.012080.

15. Morrell, S.; Taylor, R.; Roder, D.; Dobson, A. Mammography screening and breast cancer mortality in Australia: an aggregate cohort study. *J. Med. Screen.* **2012**, *19*, 26–34, doi:10.1258/jms.2012.011127.

16. Marmot, M.; Screening, T.I.U.P.O.B.C.; Altman, D.G.; Cameron, D.A.; Dewar, J.A.; Thompson, S.G.; Wilcox, M. The benefits and harms of breast cancer screening: an independent review. *Br. J. Cancer* **2013**, *108*, 2205–2240, doi:10.1038/bjc.2013.177.

17. Liu, C.-Y.; Hsu, C.-Y.; Chou, Y.-H.; Chen, C.-M. A multi-scale tumor detection algorithm in whole breast sonography incorporating breast anatomy and tissue morphological information. In Proceedings of the 2014 IEEE Healthcare Innovation Conference (HIC), Seattle, WA, USA, 8–10 October 2014; pp. 193–196.

18. Pisano, E.D.; Gatsonis, C.; Hendrick, E.; Yaffe, M.; Baum, J.K.; Acharyya, S.; Conant, E.F.; Fajardo, L.L.; Bassett, L.; D'Orsi, C.; et al. Diagnostic Performance of Digital versus Film Mammography for Breast-Cancer Screening. *N. Engl. J. Med.* **2005**, *353*, 1773–1783, doi:10.1056/nejmoa052911.

19. Carney, P.A.; Miglioretti, D.L.; Yankaskas, B.C.; Kerlikowske, K.; Rosenberg, R.; Rutter, C.M.; Geller, B.M.; Abraham, L.A.; Taplin, S.H.; Dignan, M.; et al. Individual and Combined Effects of Age, Breast Density, and Hormone Replacement Therapy Use on the Accuracy of Screening Mammography. *Ann. Intern. Med.* **2003**, *138*, 168–175, doi:10.7326/0003-4819-138-3-200302040-00008.

20. Woodard, D.B.; Gelfand, A.E.; Barlow, W.E.; Elmore, J.G. Performance assessment for radiologists interpreting screening mammography. *Stat. Med.* **2007**, *26*, 1532–1551, doi:10.1002/sim.2633.

21. Cole, E.; Pisano, E.D.; Kistner, E.O.; Muller, K.E.; Brown, M.E.; Feig, S.A.; Jong, R.A.; Maidment, A.D.A.; Staiger, M.J.; Kuzmiak, C.M.; et al. Diagnostic Accuracy of Digital Mammography in Patients with Dense Breasts Who Underwent Problem-solving Mammography: Effects of Image Processing and Lesion Type1. *Radiology.* **2003**, *226*, 153–160, doi:10.1148/radiol.2261012024.

22. Boyd, N.F.; Guo, H.; Martin, L.J.; Sun, L.; Stone, J.; Fishell, E.; Jong, R.A.; Hislop, G.; Chiarelli, A.; Minkin, S.; et al. Mammographic Density and the Risk and Detection of Breast Cancer. *N. Engl. J. Med.* **2007**, *356*, 227–236, doi:10.1056/nejmoa062790.

23. E Bird, R.; Wallace, T.W.; Yankaskas, B.C. Analysis of cancers missed at screening mammography. *Radiology* **1992**, *184*, 613–617, doi:10.1148/radiology.184.3.1509041.

24. Kerlikowske, K.; Carney, P.A.; Geller, B.; Mandelson, M.T.; Taplin, S.; Malvin, K.; Ernster, V.; Urban, N.; Cutter, G.; Rosenberg, R.; et al. Performance of screening mammography among women with and without a first-degree relative with breast cancer. *Ann. Intern. Med.* **2000**, *133*, 855–863, doi:10.7326/0003-4819-133-11-200012050-00009.

25. Ertosun, M.G.; Rubin, D.L. Probabilistic visual search for masses within mammography images using deep learning. In Proceedings of the 2015 IEEE International Conference on Bioinformatics and Biomedicine (BIBM), Washington, DC, USA, 9–12 November 2015; pp. 1310–1315.

26. Nunes, F.L.S.; Schiabel, H.; Goes, C.E. Contrast Enhancement in Dense Breast Images to Aid Clustered Microcalcifications Detection. *J. Digit. Imaging* **2006**, *20*, 53–66, doi:10.1007/s10278-005-6976-5.

27. Szegedy, C.; Vanhoucke, V.; Ioffe, S.; Shlens, J.; Wojna, Z. Rethinking the Inception Architecture for Computer Vision. In Proceedings of the 2016 IEEE Conference on Computer Vision and Pattern Recognition (CVPR), Las Vegas, NV, USA, 27–30 June 2016; pp. 2818–2826.

28. Dinnes, J.; Moss, S.; Melia, J.; Blanks, R.; Song, F.; Kleijnen, J. Effectiveness and cost-effectiveness of double reading of mammograms in breast cancer screening: findings of a systematic review. *Breast* **2001**, *10*, 455–463, doi:10.1054/brst.2001.0350.

29. Robinson, P.J. Radiology's Achilles' heel: Error and variation in the interpretation of the Röntgen image. *Br. J. Radiol.* **1997**, *70*, 1085–1098.

30. Rangayyan, R.M.; Ayres, F.J.; Desautels, J.L. A review of computer-aided diagnosis of breast cancer: Toward the detection of subtle signs. *J. Frankl. Inst.* **2007**, *344*, 312–348, doi:10.1016/j.jfranklin.2006.09.003.

31. Jalalian, A.; Mashohor, S.; Mahmud, R.; Karasfi, B.; Saripan, M.I.B.; Ramli, A.R.B. Foundation and methodologies in computer-aided diagnosis systems for breast cancer detection. *EXCLI J.* **2017**, *16*, 113–137.

32. Vyborny, C.J.; Giger, M.L.; Nishikawa, R.M. COMPUTER-AIDED DETECTION AND DIAGNOSIS OF BREAST CANCER. *Radiol. Clin. N. Am.* **2000**, *38*, 725–740, doi:10.1016/s0033-8389(05)70197-4.

33. Giger, M.L. Machine Learning in Medical Imaging. *J. Am. Coll. Radiol.* **2018**, *15*, 512–520, doi:10.1016/j.jacr.2017.12.028.

34. Xu, Y.; Wang, Y.; Yuan, J.; Cheng, Q.; Wang, X.; Carson, P.L. Medical breast ultrasound image segmentation by machine learning. *Ultrasonics* **2019**, *91*, 1–9, doi:10.1016/j.ultras.2018.07.006.

35. Shan, J.; Alam, S.K.; Garra, B.; Zhang, Y.; Ahmed, T. Computer-Aided Diagnosis for Breast Ultrasound Using Computerized BI-RADS Features and Machine Learning Methods. *Ultrasound Med. Biol.* **2016**, *42*, 980–988, doi:10.1016/j.ultrasmedbio.2015.11.016.

36. Zhang, Q.; Xiao, Y.; Dai, W.; Suo, J.; Wang, C.; Shi, J.; Zheng, H. Deep learning based classification of breast tumors with shear-wave elastography. *Ultrasonics* **2016**, *72*, 150–157, doi:10.1016/j.ultras.2016.08.004.

37. Cheng, J.-Z.; Ni, D.; Chou, Y.-H.; Qin, J.; Tiu, C.-M.; Chang, Y.-C.; Huang, C.-S.; Shen, D.; Chen, C.-M. Computer-Aided Diagnosis with Deep Learning Architecture: Applications to Breast Lesions in US Images and Pulmonary Nodules in CT Scans. *Sci. Rep.* **2016**, *6*, 24454, doi:10.1038/srep24454.

38. Shin, S.Y.; Lee, S.; Yun, I.D.; Kim, S.M.; Lee, K.M. Joint Weakly and Semi-Supervised Deep Learning for Localization and Classification of Masses in Breast Ultrasound Images. *IEEE Trans. Med. Imaging* **2018**, *38*, 762–774, doi:10.1109/tmi.2018.2872031.

39. Wang, J.; Ding, H.; Bidgoli, F.A.; Zhou, B.; Iribarren, C.; Molloi, S.; Baldi, P. Detecting Cardiovascular Disease from Mammograms With Deep Learning. *IEEE Trans. Med. Imaging* **2017**, *36*, 1172–1181, doi:10.1109/tmi.2017.2655486.

40. Dhungel, N.; Carneiro, G.; Bradley, A.P. Fully automated classification of mammograms using deep residual neural networks. In Proceedings of the 2017 IEEE 14th International Symposium on Biomedical Imaging (ISBI 2017), Melbourne, Australia, 18–21 April 2017; pp. 310–314.

41. Kooi, T.; Litjens, G.J.S.; Van Ginneken, B.; Gubern-Mérida, A.; Sánchez, C.I.; Mann, R.; Heeten, A.D.; Karssemeijer, N. Large scale deep learning for computer aided detection of mammographic lesions. *Med. Image Anal.* **2017**, *35*, 303–312, doi:10.1016/j.media.2016.07.007.

42. Debelee, T.G.; Schwenker, F.; Ibenthal, A.; Yohannes, D. Survey of deep learning in breast cancer image analysis. *Evol. Syst.* **2020**, *11*, 143–163, doi:10.1007/s12530-019-09297-2.

43. Keen, J.D.; Keen, J.M.; Keen, J.E. Utilization of computer-aided detection for digital screening mammography in the United States, 2008 to 2016. *J. Am. Coll. Radiol.* **2018**, *15*, 44–48.

44. Henriksen, E.L.; Carlsen, J.F.; Vejborg, I.; Nielsen, M.B.; A Lauridsen, C. The efficacy of using computer-aided detection (CAD) for detection of breast cancer in mammography screening: a systematic review. *Acta Radiol.* **2018**, *60*, 13–18, doi:10.1177/0284185118770917.

45. Gao, Y.; Geras, K.J.; Lewin, A.A.; Moy, L. New Frontiers: An Update on Computer-Aided Diagnosis for Breast Imaging in the Age of Artificial Intelligence. *Am. J. Roentgenol.* **2019**, *212*, 300–307, doi:10.2214/ajr.18.20392.

46. Pacilè, S.; Lopez, J.; Chone, P.; Bertinotti, T.; Grouin, J.M., Fillard, P. Improving Breast Cancer Detection Accuracy of Mammography with the Concurrent Use of an Artificial Intelligence Tool. *Radiol. Artif. Intell.* **2020**, *2*, e190208.

47. Huynh, B.Q.; Li, H.; Giger, M.L. Digital mammographic tumor classification using transfer learning from deep convolutional neural networks. *J. Med. Imaging* **2016**, *3*, 034501, doi:10.1117/1.jmi.3.3.034501.

48. Yap, M.H.; Pons, G.; Marti, J.; Ganau, S.; Sentis, M.; Zwiggelaar, R.; Davison, A.K.; Marti, R. Automated Breast Ultrasound Lesions Detection Using Convolutional Neural Networks. *IEEE J. Biomed. Heal. Inform.* **2018**, *22*, 1218–1226, doi:10.1109/jbhi.2017.2731873.

49. Moon, W.K.; Lee, Y.-W.; Ke, H.-H.; Lee, S.H.; Huang, C.-S.; Chang, R.-F. Computer-aided diagnosis of breast ultrasound images using ensemble learning from convolutional neural networks. *Comput. Methods Programs Biomed.* **2020**, *190*, 105361, doi:10.1016/j.cmpb.2020.105361.

50. Yap, M.H.; Goyal, M.; Osman, F.; Ahmad, E.; Martí, R.; Denton, E.; Juette, A.; Zwiggelaar, R. End-to-end breast ultrasound lesions recognition with a deep learning approach. In *Medical Imaging 2018: Biomedical Applications in Molecular, Structural, and Functional Imaging*; International Society for Optics and Photonics: Bellingham, WA, USA, 2018; Volume 10578, p. 1057819.

51. Xu, B.; Wang, N.; Chen, T.; Li, M. Empirical evaluation of rectified activations in convolutional network. *arXiv* **2015**, arXiv:1505.00853.

52. Swiderski, B.; Kurek, J.; Osowski, S.; Kruk, M.; Barhoumi, W. Deep learning and non-negative matrix factorization in recognition of mammograms. In Proceedings of the Eighth International Conference on Graphic and Image Processing (ICGIP 2016), Tokyo, Japan, 29–31 October 2016; International Society for Optics and Photonics: Bellingham, WA, USA, 2017; Volume 10225, p. 102250B.

53. Lecun, Y.; Bengio, Y.; Hinton, G. Deep learning. *Nature* **2015**, *521*, 436–444.

54. Miotto, R.; Wang, F.; Wang, S.; Jiang, X.; Dudley, J.T. Deep learning for healthcare: review, opportunities and challenges. *Briefings Bioinform.* **2018**, *19*, 1236–1246, doi:10.1093/bib/bbx044.

55. Shin, H.-C.; Roth, H.R.; Gao, M.; Lu, L.; Xu, Z.; Nogues, I.; Yao, J.; Mollura, D.; Summers, R.M. Deep Convolutional Neural Networks for Computer-Aided Detection: CNN Architectures, Dataset Characteristics and Transfer Learning. *IEEE Trans. Med. Imaging* **2016**, *35*, 1285–1298, doi:10.1109/tmi.2016.2528162.

56. Lee, J.-G.; Jun, S.; Cho, Y.-W.; Lee, H.; Kim, G.B.; Seo, J.B.; Kim, N. Deep Learning in Medical Imaging: General Overview. *Korean J. Radiol.* **2017**, *18*, 570–584, doi:10.3348/kjr.2017.18.4.570.

57. Suzuki, K. Overview of deep learning in medical imaging. *Radiol. Phys. Technol.* **2017**, *10*, 257–273, doi:10.1007/s12194-017-0406-5.

58. Moradmand, H.; Setayeshi, S.; Karimian, A.R.; Sirous, M.; Akbari, M.E. Comparing the performance of image enhancement methods to detect microcalcification clusters in digital mammography. *Iran. J. Cancer Prev.* **2012**, *5*, 61.

59. Moher, D.; Liberati, A.; Tetzlaff, J.; Altman, D.G. Preferred reporting items for systematic reviews and meta-analyses: The PRISMA statement. *Int. J. Surg.* **2010**, *8*, 336–341, doi:10.1016/j.ijsu.2010.02.007.

60. Khan, K.S.; Kunz, R.; Kleijnen, J.; Antes, G. Five steps to conducting a systematic review. *J. R. Soc. Med.* **2003**, *96*, 118–121.

61. Suckling J, P. The mammographic image analysis society digital mammogram database. *Digit. Mammo.* **1994**, *1069*, 375–386.

62. Han, S.; Kang, H.-K.; Jeong, J.-Y.; Park, M.-H.; Kim, W.; Bang, W.-C.; Seong, Y.-K. A deep learning framework for supporting the classification of breast lesions in ultrasound images. *Phys. Med. Biol.* **2017**, *62*, 7714–7728, doi:10.1088/1361-6560/aa82ec.

63. De Oliveira, J.E.; Deserno, T.M.; Araújo, A.D.A. Breast Lesions Classification applied to a reference database. In Proceedings of the 2nd International Conference, Hammanet, Tunisia, 29–31 October 2008; pp. 29–31.

64. Moreira, I.C.; Amaral, I.; Domingues, I.; Cardoso, A.; Cardoso, M.J.; Cardoso, J.S. Inbreast: Toward a full-field digital mammographic database. *Acad. Radiol.* **2012**, *19*, 236–248.

65. Abdelhafiz, D.; Yang, C.; Ammar, R.; Nabavi, S. Deep convolutional neural networks for mammography: advances, challenges and applications. *BMC Bioinform.* **2019**, *20*, 281, doi:10.1186/s12859-019-2823-4.

66. Byra, M.; Jarosik, P.; Szubert, A.; Galperin, M.; Ojeda-Fournier, H.; Olson, L.; O'Boyle, M.; Comstock, C.; Andre, M. Breast mass segmentation in ultrasound with selective kernel U-Net convolutional neural network. *Biomed. Signal. Process. Control.* **2020**, *61*, 102027, doi:10.1016/j.bspc.2020.102027.

67. Jiao, Z.; Gao, X.; Wang, Y.; Li, J. A deep feature based framework for breast masses classification. *Neurocomputing* **2016**, *197*, 221–231, doi:10.1016/j.neucom.2016.02.060.

68. Arevalo, J.; González, F.A.; Ramos-Pollán, R.; Oliveira, J.L.; Lopez, M.A.G. Representation learning for mammography mass lesion classification with convolutional neural networks. *Comput. Methods Programs Biomed.* **2016**, *127*, 248–257, doi:10.1016/j.cmpb.2015.12.014.

69. Peng, W.; Mayorga, R.; Hussein, E. An automated confirmatory system for analysis of mammograms. *Comput. Methods Programs Biomed.* **2016**, *125*, 134–144, doi:10.1016/j.cmpb.2015.09.019.

70. Dhabyani, W.; Gomaa, M.; Khaled, H.; Fahmy, A. Dataset of breast ultrasound images. *Data Brief.* **2020**, *28*, 104863, doi:10.1016/j.dib.2019.104863.

71. Tian, J.-W.; Wang, Y.; Huang, J.-H.; Ning, C.-P.; Wang, H.-M.; Liu, Y.; Tang, X.-L. The Digital Database for Breast Ultrasound Image. In *Proceedings of 11th Joint Conference on Information Sciences (JCIS)*; Atlantis Press: Amsterdam, The Netherlands, 2008.

72. Piotrzkowska-Wróblewska, H.; Dobruch-Sobczak, K.; Byra, M.; Nowicki, A. Open access database of raw ultrasonic signals acquired from malignant and benign breast lesions. *Med. Phys.* **2017**, *44*, 6105–6109, doi:10.1002/mp.12538.

73. Deng, J.; Dong, W.; Socher, R.; Li, L.J.; Li, K.; Fei-Fei, L. Imagenet: A large-scale hierarchical image database. In Proceedings of the 2009 IEEE Conference on Computer Vision and Pattern Recognition, Miami, FL, USA, 20–25 June 2009; pp. 248-255.

74. Fujita, H. AI-based computer-aided diagnosis (AI-CAD): the latest review to read first. *Radiol. Phys. Technol.* **2020**, *13*, 6–19, doi:10.1007/s12194-019-00552-4.

75. Sengupta, S.; Singh, A.; Leopold, H.A.; Gulati, T.; Lakshminarayanan, V. Ophthalmic diagnosis using deep learning with fundus images—A critical review. *Artif. Intell. Med.* **2020**, *102*, 101758, doi:10.1016/j.artmed.2019.101758.

76. Shih, F.Y. *Image Processing and Pattern Recognition: Fundamentals and Techniques*; John Wiley & Sons: Hoboken, NJ, USA, 2010.

77. Biltawi, M., Al-Najdawi, N.I.J.A.D., & Tedmori, S.A.R.A. Mammogram enhancement and segmentation methods: classification, analysis, and evaluation. In Proceeding of the 13th International Arab Conference on Information Technology, Zarqa, Jordan, 10–13 December 2012

78. Dabass, J.; Arora, S.; Vig, R.; Hanmandlu, M. Segmentation techniques for breast cancer imaging modalities—A review. In Proceedings of the 2019 9th International Conference on Cloud Computing, Data Science & Engineering (Confluence), Noida, India, 10–11 January 2019; pp. 658–663.

79. Ganesan, K.; Acharya, U.R.; Chua, K.C.; Min, L.C.; Abraham, K.T. Pectoral muscle segmentation: A review. *Comput. Methods Programs Biomed.* **2013**, *110*, 48–57, doi:10.1016/j.cmpb.2012.10.020.

80. Huang, Q.; Luo, Y.; Zhang, Q. Breast ultrasound image segmentation: a survey. *Int. J. Comput. Assist. Radiol. Surg.* **2017**, *12*, 493–507, doi:10.1007/s11548-016-1513-1.

81. Noble, J.A.; Boukerroui, D. Ultrasound image segmentation: A survey. *IEEE Trans. Med. Imaging* **2006**, *25*, 987–1010, doi:10.1109/tmi.2006.877092.

82. Kallergi, M; Woods, K.; Clarke, L.P.; Qian, W.; Clark, R.A. Image segmentation in digital mammography: Comparison of local thresholding and region growing algorithms. *Comput. Med. Imaging Graph.* **1992**, *16*, 323–331, doi:10.1016/0895-6111(92)90145-y.

83. Tsantis, S.; Dimitropoulos, N.; Cavouras, D.; Nikiforidis, G. A hybrid multi-scale model for thyroid nodule boundary detection on ultrasound images. *Comput. Methods Programs Biomed.* **2006**, *84*, 86–98, doi:10.1016/j.cmpb.2006.09.006.

84. Ilesanmi, A.E.; Idowu, O.P.; Makhanov, S.S. Multiscale superpixel method for segmentation of breast ultrasound. *Comput. Biol. Med.* **2020**, *125*, 103879, doi:10.1016/j.compbiomed.2020.103879.

85. Chen, D.; Chang, R.-F.; Kuo, W.-J.; Chen, M.-C.; Huang, Y.-L. Diagnosis of breast tumors with sonographic texture analysis using wavelet transform and neural networks. *Ultrasound Med. Biol.* **2002**, *28*, 1301–1310, doi:10.1016/s0301-5629(02)00620-8.

86. Cheng, H.D.; Shan, J.; Ju, W.; Guo, Y.; Zhang, L. Automated breast cancer detection and classification using ultrasound images: A survey. *Pattern Recognit.* **2010**, *43*, 299–317, doi:10.1016/j.patcog.2009.05.012.

87. Hasan, H.; Tahir, N.M. Feature selection of breast cancer based on principal component analysis. In Proceedings of the 2010 6th International Colloquium on Signal Processing & Its Applications, Mallaca City, Malaysia, 21–23 May 2010; pp. 1–4.

88. Chan, H.-P.; Wei, D.; A Helvie, M.; Sahiner, B.; Adler, D.D.; Goodsitt, M.M.; Petrick, N. Computer-aided classification of mammographic masses and normal tissue: linear discriminant analysis in texture feature space. *Phys. Med. Biol.* **1995**, *40*, 857–876, doi:10.1088/0031-9155/40/5/010.

89. Maglogiannis, I.; Zafiropoulos, E.; Kyranoudis, C. Intelligent segmentation and classification of pigmented skin lesions in dermatological images. In *Hellenic Conference on Artificial Intelligence*; Springer: Berlin/Heidelberg, Germany, 2006; pp. 214–223.

90. Jin, X.; Xu, A.; Bie, R.; Guo, P. Machine learning techniques and chi-square feature selection for cancer classification using SAGE gene expression profiles. In *International Workshop on Data Mining for Biomedical Applications;* Springer: Berlin/Heidelberg, Germany, 2006; pp. 106–115.

91. Verma, K.; Singh, B.K.; Tripathi, P.; Thoke, A.S. Review of feature selection algorithms for breast cancer ultrasound image. In *New Trends in Intelligent Information and Database Systems*; Springer: Cham, Switzerland, 2015; pp. 23-32.

92. Sikorski, J. Identification of malignant melanoma by wavelet analysis. In Proceedings of the Student/Faculty Research Day, CSIS, Pace University New York, NY, USA, 7 May 2004.

93. Chiem, A.; Al-Jumaily, A.; Khushaba, R.N. A novel hybrid system for skin lesion detection. In Proceedings of the 2007 3rd International Conference on Intelligent Sensors, Sensor Networks and Information, Melbourne, Australia, 3–6 December 2007; pp. 567–572.

94. Tanaka, T.; Torii, S.; Kabuta, I.; Shimizu, K.; Tanaka, M. Pattern Classification of Nevus with Texture Analysis. *IEEJ Trans. Electr. Electron. Eng.* **2007**, *3*, 143–150, doi:10.1002/tee.20246.

95. Zhou, H.; Chen, M.; Rehg, J.M. Dermoscopic interest point detector and descriptor. In Proceedings of the 2009 IEEE International Symposium on Biomedical Imaging: From Nano to Macro, Boston, MA, USA, 28 June–1 July 2009; pp. 1318–1321.

96. Singh, B.; Jain, V.K.; Singh, S. Mammogram Mass Classification Using Support Vector Machine with Texture, Shape Features and Hierarchical Centroid Method. *J. Med. Imaging Heal. Informatics* **2014**, *4*, 687–696, doi:10.1166/jmihi.2014.1312.

97. Sonar, P.; Bhosle, U.; Choudhury, C. Mammography classification using modified hybrid SVM-KNN. In Proceedings of the 2017 International Conference on Signal Processing and Communication (ICSPC), Coimbatore, India, 28–29 July 2017; pp. 305–311.

98. Pal, N.R.; Bhowmick, B.; Patel, S.K.; Pal, S.; Das, J. A multi-stage neural network aided system for detection of microcalcifications in digitized mammograms. *Neurocomputing* **2008**, *71*, 2625–2634, doi:10.1016/j.neucom.2007.06.015.

99. Ayer, T.; Chen, Q.; Burnside, E.S. Artificial Neural Networks in Mammography Interpretation and Diagnostic Decision Making. *Comput. Math. Methods Med.* **2013**, *2013*, 1–10, doi:10.1155/2013/832509.

100. Al-Hadidi, M.R.; Alarabeyyat, A.; Alhanahnah, M. Breast cancer detection using k-nearest neighbor machine learning algorithm. In Proceedings of the 2016 9th International Conference on Developments in eSystems Engineering (DeSE), Liverpool, UK, 31 August–2 September 2016; pp. 35–39.

101. Sumbaly, R.; Vishnusri, N.; Jeyalatha, S. Diagnosis of Breast Cancer using Decision Tree Data Mining Technique. *Int. J. Comput. Appl.* **2014**, *98*, 16–24, doi:10.5120/17219-7456.

102. Landwehr, N.; Hall, M.A.; Frank, E. Logistic Model Trees. *Mach. Learn.* **2005**, *59*, 161–205, doi:10.1007/s10994-005-0466-3.

103. Abdel-Zaher, A.M.; Eldeib, A.M. Breast cancer classification using deep belief networks. *Expert Syst. Appl.* **2016**, *46*, 139–144, doi:10.1016/j.eswa.2015.10.015.

104. Nishikawa, R.M.; Giger, M.L.; Doi, K.; Metz, C.E.; Yin, F.-F.; Vyborny, C.J.; Schmidt, R.A. Effect of case selection on the performance of computer-aided detection schemes. *Med. Phys.* **1994**, *21*, 265–269, doi:10.1118/1.597287.

105. Rodríguez-Ruiz, A.; Teuwen, J.; Chung, K.; Karssemeijer, N.; Chevalier, M.; Gubern-Merida, A.; Sechopoulos, I. Pectoral muscle segmentation in breast tomosynthesis with deep learning. In *Medical Imaging 2018: Computer-Aided Diagnosis*; International Society for Optics and Photonics: Bellingham, WA, USA, 2018; Volume 10575, p. 105752J.

106. Guo, R.; Lu, G.; Qin, B.; Fei, B. Ultrasound Imaging Technologies for Breast Cancer Detection and Management: A Review. *Ultrasound Med. Biol.* **2018**, *44*, 37–70, doi:10.1016/j.ultrasmedbio.2017.09.012.

107. Cadena, L.; Castillo, D.; Zotin, A.; Diaz, P.; Cadena, F.; Cadena, G.; Jimenez, Y. (2019) Processing MRI Brain Image using OpenMP and Fast Filters for Noise Reduction. In Proceedings of the World Congress on Engineering and Computer Science 2019, San Francisco, CA, USA, 22–24 October 2019.

108. Kang, C.-C.; Wang, W.-J.; Kang, C.-H. Image segmentation with complicated background by using seeded region growing. *AEU—Int. J. Electron. Commun.* **2012**, *66*, 767–771, doi:10.1016/j.aeue.2012.01.011.

109. Prabusankarlal, K.M.; Thirumoorthy, P.; Manavalan, R. Computer Aided Breast Cancer Diagnosis Techniques in Ultrasound: A Survey. *J. Med. Imaging Health Inform.* **2014**, *4*, 331–349, doi:10.1166/jmihi.2014.1269.

110. Abdallah, Y.M.Y.; Elgak, S.; Zain, H.; Rafiq, M.; Ebaid, E.A.; Elnaema, A.A. Breast cancer detection using image enhancement and segmentation algorithms. *Biomed. Res.* **2018**, *29*, 3732–3736, doi:10.4066/biomedicalresearch.29-18-1106.

111. Sheba, K.U.; Gladston Raj, S. Objective Quality Assessment of Image Enhancement Methods in Digital Mammography - A Comparative Study. *Signal. Image Process. Int. J.* **2016**, *7*, 1–13, doi:10.5121/sipij.2016.7401.

112. George, M.J.; Sankar, S.P. Efficient preprocessing filters and mass segmentation techniques for mammogram images. In Proceedings of the 2017 IEEE International Conference on Circuits and Systems (ICCS), Thiruvananthapuram, India, 20–21 December 2017; pp. 408–413.

113. Talha, M.; Sulong, G.B.; Jaffar, A. Preprocessing digital breast mammograms using adaptive weighted frost filter. *Biomed. Res.* **2016**, *27*, 1407–1412.

114. Thitivirut, M.; Leekitviwat, J.; Pathomsathit, C.; Phasukkit, P. Image Enhancement by using Triple Filter and Histogram Equalization for Organ Segmentation. In Proceedings of the 2019 12th Biomedical Engineering International Conference (BMEiCON), Ubon Ratchathani, Thailand, 19–22 November 2019; pp. 1–5.

115. Gandhi, K.R.; Karnan, M. Mammogram image enhancement and segmentation. In Proceedings of the IEEE International Conference on Computational Intelligence and Computing Research (ICCIC), Coimbatore, India, 28–29 December 2010; pp. 1–4.

116. Pizer, S.M.; Amburn, E.P.; Austin, J.D.; Cromartie, R.; Geselowitz, A.; Greer, T.; Romeny, B.M.T.H.; Zimmerman, J.B.; Zuiderveld, K.K. Adaptive histogram equalization and its variations. *Comput. Vision Graph. Image Process.* **1987**, *39*, 355–368, doi:10.1016/s0734-189x(87)80186-x.

117. Pisano, E.D.; Zong, S.; Hemminger, B.M.; DeLuca, M.; Johnston, R.E.; Muller, K.; Braeuning, M.P.; Pizer, S.M. Contrast Limited Adaptive Histogram Equalization image processing to improve the detection of simulated spiculations in dense mammograms. *J. Digit. Imaging* **1998**, *11*, 193–200, doi:10.1007/bf03178082.

118. Wan, J.; Yin, H.; Chong, A.-X.; Liu, Z.-H. Progressive residual networks for image super-resolution. *Appl. Intell.* **2020**, *50*, 1620–1632, doi:10.1007/s10489-019-01548-8.

119. Umehara, K.; Ota, J.; Ishida, T. Super-Resolution Imaging of Mammograms Based on the Super-Resolution Convolutional Neural Network. *Open J. Med. Imaging* **2017**, *7*, 180–195, doi:10.4236/ojmi.2017.74018.

120. Dong, C.; Loy, C.C.; He, K.; Tang, X. Image Super-Resolution Using Deep Convolutional Networks. *IEEE Trans. Pattern Anal. Mach. Intell.* **2015**, *38*, 295–307, doi:10.1109/tpami.2015.2439281.

121. Kim, J.; Lee, J.K.; Lee, K.M. Accurate image super-resolution using very deep convolutional networks. In Proceedings of the IEEE Conference on Computer Vision and Pattern Recognition, Las Vegas, NV, USA, 27–30 June 2016; pp. 1646–1654.

122. Jiang, Y.; Li, J. Generative Adversarial Network for Image Super-Resolution Combining Texture Loss. *Appl. Sci.* **2020**, *10*, 1729, doi:10.3390/app10051729.

123. Glasner, D.; Bagon, S.; Irani, M. Super-resolution from a single image. In Proceedings of the 2009 IEEE 12th International Conference on Computer Vision, Kyoto, Japan, 29 September–2 October 2009; pp. 349–356.

124. Schultz, R.; Stevenson, R.; R.R., S.; R.L., S. A Bayesian approach to image expansion for improved definition. *IEEE Trans. Image Process.* **1994**, *3*, 233–242, doi:10.1109/83.287017.

125. Gribbon, K.T.; Bailey, D.G. A novel approach to real-time bilinear interpolation. In Proceedings of the DELTA 2004 Second IEEE International Workshop on Electronic Design, Test and Applications, Perth, Australia, 28–30 January 2004; pp. 126–131.

126. Zhang, L.; Wu, X. An edge-guided image interpolation algorithm via directional filtering and data fusion. *IEEE Trans. Image Process.* **2006**, *15*, 2226–2238, doi:10.1109/tip.2006.877407.

127. Sun, C.; Shrivastava, A.; Singh, S.; Gupta, A. Revisiting unreasonable effectiveness of data in deep learning era. In Proceedings of the IEEE International Conference on Computer Vision, Venice, Italy, 22–29 October 2017; pp. 843–852.

128. Shorten, C.; Khoshgoftaar, T.M. A survey on Image Data Augmentation for Deep Learning. *J. Big Data* **2019**, *6*, 60, doi:10.1186/s40537-019-0197-0.

129. Weiss, K.; Khoshgoftaar, T.M.; Wang, D. A survey of transfer learning. *J. Big Data* **2016**, *3*, 1, doi:10.1186/s40537-016-0043-6.

130. Shao, L.; Zhu, F.; Li, X. Transfer Learning for Visual Categorization: A Survey. *IEEE Trans. Neural Networks Learn. Syst.* **2015**, *26*, 1019–1034, doi:10.1109/tnnls.2014.2330900.

131. Zhong, Z.; Zheng, L.; Kang, G.; Li, S.; Yang, Y. Random Erasing Data Augmentation. In Proceedings of the AAAI Conference on Artificial Intelligence, New York, New York, USA, 7–12 February 2020; pp. 13001–13008.

132. Mirza, M.; Osindero, S. Conditional Generative Adversarial Nets Mehdi. *arXiv* **2014**, arxiv:1411.1784.

133. Gatys, L.; Ecker, A.; Bethge, M. A Neural Algorithm of Artistic Style. *J. Vis.* **2016**, *16*, 326, doi:10.1167/16.12.326.

134. Mordang, J.-J.; Janssen, T.; Bria, A.; Kooi, T.; Gubern-Mérida, A.; Karssemeijer, N. Automatic Microcalcification Detection in Multi-vendor Mammography Using Convolutional Neural Networks. In *Public-Key Cryptography—PKC 2018*; Springer Science and Business Media LLC: New York, NY, USA, 2016; pp. 35–42.

135. Akselrod-Ballin, A.; Karlinsky, L.; Alpert, S.; Hasoul, S.; Ben-Ari, R.; Barkan, E. A region based convolutional network for tumor detection and classification in breast mammography. In *Deep Learning and Data Labeling for Medical Applications*; Springer: Cham, Switzerland, 2016; pp. 197–205.

136. Zhu, W.; Xie, X. Adversarial Deep Structural Networks for Mammographic Mass Segmentation. *arXiv* **2016**, arXiv:1612.05970.

137. Lévy, D.; Jain, A. Breast mass classification from mammograms using deep convolutional neural networks. *arXiv* **2016**, arXiv:1612.00542.

138. Sert, E.; Ertekin, S.; Halici, U. Ensemble of convolutional neural networks for classification of breast microcalcification from mammograms. In Proceedings of the 2017 39th Annual International Conference of the IEEE Engineering in Medicine and Biology Society (EMBC), Seogwipo, Korea, 11–15 July 2017; pp. 689–692.

139. Dhungel, N.; Carneiro, G.; Bradley, A.P. The automated learning of deep features for breast mass classification from mammograms. In *International Conference on Medical Image Computing and Computer-Assisted Intervention*; Springer: Cham, Switzerland, 2016; pp. 106–114.

140. Saeed, J.N. A SURVEY OF ULTRASONOGRAPHY BREAST CANCER IMAGE SEGMENTATION TECHNIQUES. *Acad. J. Nawroz Univ.* **2020**, *9*, 1–14, doi:10.25007/ajnu.v9n1a523.

141. Gardezi, S.J.S.; ElAzab, A.; Lei, B.; Wang, T. Breast Cancer Detection and Diagnosis Using Mammographic Data: Systematic Review. *J. Med. Internet Res.* **2019**, *21*, e14464, doi:10.2196/14464.

142. Gomez, W.; Rodriguez, A.; Pereira, W.C.A.; Infantosi, A.F.C. Feature selection and classifier performance in computer-aided diagnosis for breast ultrasound. In Proceedings of the 2013 10th International Conference and Expo on Emerging Technologies for a Smarter World (CEWIT), Melville, NY, USA, 21–22 October 2013; pp. 1–5.

143. Dong, C.; Loy, C.C.; He, K.; Tang, X. Learning a deep convolutional network for image super-resolution. In *European Conference on Computer Vision*; Springer: Cham, Switzerland, 2014; pp. 184–199.

144. Lotter, W.; Sorensen, G.; Cox, D. A multi-scale CNN and curriculum learning strategy for mammogram classification. In *Deep Learning in Medical Image Analysis and Multimodal Learning for Clinical Decision Support*; Springer: Cham, Switzerland, 2017; pp. 169–177.

145. Al-Masni, M.A.; Al-Antari, M.A.; Park, J.-M.; Gi, G.; Kim, T.-S.; Rivera, P.; Valarezo, E.; Choi, M.-T.; Han, S.-M. Simultaneous detection and classification of breast masses in digital mammograms via a deep learning YOLO-based CAD system. *Comput. Methods Programs Biomed.* **2018**, *157*, 85–94, doi:10.1016/j.cmpb.2018.01.017.

146. Badrinarayanan, V.; Kendall, A.; Cipolla, R. SegNet: A Deep Convolutional Encoder-Decoder Architecture for Image Segmentation. *IEEE Trans. Pattern Anal. Mach. Intell.* **2017**, *39*, 2481–2495, doi:10.1109/tpami.2016.2644615.

147. Almajalid, R.; Shan, J.; Du, Y.; Zhang, M. Development of a deep-learning-based method for breast ultrasound image segmentation. In Proceedings of the 2018 17th IEEE International Conference on Machine Learning and Applications (ICMLA), Orlando, FL, USA, 17–20 December 2018; pp. 1103–108.

148. Ronneberger, O.; Fischer, P.; Brox, T. U-net: Convolutional networks for biomedical image segmentation. In *Proceedings of the Lecture Notes in Computer Science*; (including subseries Lecture Notes in Artificial Intelligence and Lecture Notes in Bioinformatics); Springer: Berlin/Heidelberg, Germany, 2015.

149. Kim, T.; Cha, M.; Kim, H.; Lee, J.K.; Kim, J. Learning to discover cross-domain relations with generative adversarial networks. *arXiv* **2017**, arXiv:1703.05192.

150. Romera, E.; Alvarez, J.M.; Bergasa, L.M.; Arroyo, R. ERFNet: Efficient Residual Factorized ConvNet for Real-Time Semantic Segmentation. *IEEE Trans. Intell. Transp. Syst.* **2018**, *19*, 263–272, doi:10.1109/tits.2017.2750080.

151. Lee, C.; Landgrebe, D. Feature extraction based on decision boundaries. *IEEE Trans. Pattern Anal. Mach. Intell.* **1993**, *15*, 388–400, doi:10.1109/34.206958.

152. Cao, Z.; Duan, L.; Yang, G.; Yue, T.; Chen, Q. An experimental study on breast lesion detection and classification from ultrasound images using deep learning architectures. *BMC Med. Imaging* **2019**, *19*, 1–9, doi:10.1186/s12880-019-0349-x.

153. Chiao, J.-Y.; Chen, K.-Y.; Liao, K.Y.-K.; Hsieh, P.-H.; Zhang, G.; Huang, T.-C. Detection and classification the breast tumors using mask R-CNN on sonograms. *Medicine* **2019**, *98*, e15200, doi:10.1097/md.0000000000015200.

154. Dhungel, N.; Carneiro, G.; Bradley, A.P. Automated Mass Detection in Mammograms Using Cascaded Deep Learning and Random Forests. In Proceedings of the 2015 International Conference on Digital Image Computing: Techniques and Applications (DICTA), Adelaide, Australia, 23–25 November 2015; pp. 1–8.

155. Hu, F.; Xia, G.-S.; Hu, J.; Zhang, L. Transferring Deep Convolutional Neural Networks for the Scene Classification of High-Resolution Remote Sensing Imagery. *Remote Sens.* **2015**, *7*, 14680–14707, doi:10.3390/rs71114680.

156. Zhu, W.; Lou, Q.; Vang, Y.S.; Xie, X. Deep multi-instance networks with sparse label assignment for whole mammogram classification. In *International Conference on Medical Image Computing and Computer-Assisted Intervention*; Springer: Cham, Switzerland, 2017; pp. 603–611.

157. Kooi, T.; Gubern-Merida, A.; Mordang, J.-J.; Mann, R.; Pijnappel, R.; Schuur, K.; Heeten, A.D.; Karssemeijer, N. A comparison between a deep convolutional neural network and radiologists for classifying regions of interest in mammography. In *International Workshop on Breast Imaging*; Springer: Cham, Switzerland, 2016; pp. 51–56.

158. Kooi, T.; Van Ginneken, B.; Karssemeijer, N.; Heeten, A.D. Discriminating solitary cysts from soft tissue lesions in mammography using a pretrained deep convolutional neural network. *Med. Phys.* **2017**, *44*, 1017–1027, doi:10.1002/mp.12110.

159. Chan, H.-P.; Lo, S.-C.B.; Sahiner, B.; Lam, K.L.; Helvie, M.A. Computer-aided detection of mammographic microcalcifications: Pattern recognition with an artificial neural network. *Med. Phys.* **1995**, *22*, 1555–1567, doi:10.1118/1.597428.

160. Valvano, G.; Della Latta, D.; Martini, N.; Santini, G.; Gori, A.; Iacconi, C.; Ripoli, A.; Landini, L.; Chiappino, D.; Iacconi, C. Evaluation of a Deep Convolutional Neural Network method for the segmentation of breast microcalcifications in Mammography Imaging. In *Precision Medicine Powered by pHealth and Connected Health*; Springer Science and Business Media LLC: New York, NY, USA, 2017; Volume 65, pp. 438–441.

161. Carneiro, G.; Nascimento, J.; Bradley, A.P. Unregistered multiview mammogram analysis with pre-trained deep learning models. In *International Conference on Medical Image Computing and Computer-Assisted Intervention*; Springer: Cham, Switzerland, 2015; pp. 652–660.

162. Carneiro, G.; Nascimento, J.; Bradley, A.P. Automated Analysis of Unregistered Multi-View Mammograms With Deep Learning. *IEEE Trans. Med. Imaging* **2017**, *36*, 2355–2365, doi:10.1109/tmi.2017.2751523.

163. LeCun, Y.; Bottou, L.; Bengio, Y.; Haffner, P. Gradient-based learning applied to document recognition. *Proc. IEEE* **1998**, *86*, 2278–2324.

164. Huynh, B.; Drukker, K.; Giger, M. MO-DE-207B-06: Computer-Aided Diagnosis of Breast Ultrasound Images Using Transfer Learning From Deep Convolutional Neural Networks. *Med. Phys.* **2016**, *43*, 3705, doi:10.1118/1.4957255.

165. Singh, V.K.; Rashwan, H.A.; Abdel-Nasser, M.; Sarker, M.; Kamal, M.; Akram, F.; Pandey, N.; Romani, S.; Puig, D. An Efficient Solution for Breast Tumor Segmentation and Classification in Ultrasound Images using Deep Adversarial Learning. *arXiv* **2019**, arXiv:1907.00887.

166. Long, J.; Shelhamer, E.; Darrell, T. Fully convolutional networks for semantic segmentation. In Proceedings of the IEEE Conference on Computer Vision and Pattern Recognition, Boston, MA, USA, 7–12 June 2015; pp. 3431–3440.

167. Liu, Y.; Yao, X. Ensemble learning via negative correlation. *Neural Networks* **1999**, *12*, 1399–1404, doi:10.1016/s0893-6080(99)00073-8.

168. Ragab, D.A.; Sharkas, M.; Marshall, S.; Ren, J. Breast cancer detection using deep convolutional neural networks and support vector machines. *PeerJ* **2019**, *7*, e6201, doi:10.7717/peerj.6201.

169. Krizhevsky, A.; Sutskever, I.; Hinton, G.E. Imagenet classification with deep convolutional neural networks. In Proceedings of the Advances in Neural Information Processing Systems, Lake Tahoe, NV, USA, 3–6 December 2012; pp. 1097–1105.

170. Simonyan, K.; Zisserman, A. Very deep convolutional networks for large-scale image recognition. *arXiv* **2014**, arXiv:1409.1556.

171. He, K.; Zhang, X.; Ren, S.; Sun, J. Deep Residual Learning for Image Recognition. *arXiv* **2015,** arXiv:1512.03385.

172. Huang, G.; Liu, Z.; van der Maaten, L.; Weinberger, K.Q. Densely Connected Convolutional Networks. In Proceedings of the IEEE Conference on Computer Vision and Pattern Recognition, Honolulu, HI, USA, 21–26 July 2017; Volume 2017, pp. 2261–2269.

173. Russakovsky, O.; Deng, J.; Su, H.; Krause, J.; Satheesh, S.; Ma, S.; Huang, Z.; Karpathy, A.; Khosla, A.; Bernstein, M.; et al. ImageNet Large Scale Visual Recognition Challenge. *Int. J. Comput. Vis.* **2015**, *115*, 211–252, doi:10.1007/s11263-015-0816-y.

174. Samala, R.K.; Chan, H.-P.; Hadjiiski, L.; Helvie, M.A.; Wei, J.; Cha, K. Mass detection in digital breast tomosynthesis: Deep convolutional neural network with transfer learning from mammography. *Med. Phys.* **2016**, *43*, 6654–6666, doi:10.1118/1.4967345.

175. Das, K.; Conjeti, S.; Roy, A.G.; Chatterjee, J.; Sheet, D. Multiple instance learning of deep convolutional neural networks for breast histopathology whole slide classification. In Proceedings of the 2018 IEEE 15th International Symposium on Biomedical Imaging (ISBI 2018), Washington, DC, USA, 4–7 April 2018; pp. 578–581.

176. Geras, K.J.; Wolfson, S.; Shen, Y.; Wu, N.; Kim, S.; Kim, E.; Heacock, L.; Parikh, U.; Moy, L.; Cho, K. High-resolution breast cancer screening with multi-view deep convolutional neural networks. *arXiv* **2017**, arXiv:1703.07047.

177. Rumelhart, D.E.; Hinton, G.E.; Williams, R.J. Learning Internal Representations by Error Propagation. In *Parallel Distributed Processing: Explorations in the Microstructure of Cognition*; MIT Press: Cambridge, MA, USA, 1985.

178. Dhungel, N.; Carneiro, G.; Bradley, A.P. A deep learning approach for the analysis of masses in mammograms with minimal user intervention. *Med. Image Anal.* **2017**, *37*, 114–128, doi:10.1016/j.media.2017.01.009.

179. Rodrigues, P.S. Breast Ultrasound Image. Mendeley Data, 1. 2017. Available online: https://data.mendeley.com/datasets/wmy84gzngw/1 (accessed on 8 October 2020).

180. Duggento, A.; Aiello, M.; Cavaliere, C.; Cascella, G.L.; Cascella, D.; Conte, G.; Guerrisi, M.; Toschi, N. An Ad Hoc Random Initialization Deep Neural Network Architecture for Discriminating Malignant Breast Cancer Lesions in Mammographic Images. *Contrast Media Mol. Imaging* **2019**, *2019*, 5982834–9, doi:10.1155/2019/5982834.

181. Chougrad, H.; Zouaki, H.; Alheyane, O. Deep Convolutional Neural Networks for breast cancer screening. *Comput. Methods Programs Biomed.* **2018**, *157*, 19–30, doi:10.1016/j.cmpb.2018.01.011.

182. Byra, M.; Sznajder, T.; Korzinek, D.; Piotrzkowska-Wroblewska, H.; Dobruch-Sobczak, K.; Nowicki, A.; Marasek, K. Impact of Ultrasound Image Reconstruction Method on Breast Lesion Classification with Deep Learning. In *Public-Key Cryptography—PKC 2018*; Springer International Publishing: Cham, Switzerland, 2019, 41–52.

183. Dheeba, J.; Singh, N.A.; Selvi, S.T. Computer-aided detection of breast cancer on mammograms: A swarm intelligence optimized wavelet neural network approach. *J. Biomed. Inform.* **2014**, *49*, 45–52, doi:10.1016/j.jbi.2014.01.010.

184. Trivizakis, E.; Ioannidis, G.S.; Melissianos, V.D.; Papadakis, G.Z.; Tsatsakis, A.; Spandidos, D.A.; Marias, K. A novel deep learning architecture outperforming 'off-the-shelf' transfer learning and feature-based methods in the automated assessment of mammographic breast density. *Oncol. Rep.* **2019**, *42*, 2009–2015, doi:10.3892/or.2019.7312.

185. Samala, R.K.; Chan, H.-P.; Hadjiiski, L.M.; Helvie, M.A.; Richter, C.; Cha, K.H. Cross-domain and multi-task transfer learning of deep convolutional neural network for breast cancer diagnosis in digital breast tomosynthesis. In *Medical Imaging 2018: Computer-Aided Diagnosis*; International Society for Optics and Photonics: Bellingham, WA, USA, 2018; Volume 10575, p. 105750Q.

186. Jadoon, M.M.; Zhang, Q.; Haq, I.U.; Butt, S.; Jadoon, A. Three-Class Mammogram Classification Based on Descriptive CNN Features. *BioMed. Res. Int.* **2017**, *2017*, 1–11, doi:10.1155/2017/3640901.

187. Ahmed, A.H.; Salem, M.A.-M. Mammogram-Based cancer detection using deep convolutional neural networks. In Proceedings of the 2018 13th International Conference on Computer Engineering and Systems (ICCES), Cairo, Egypt, 18–19 December 2018; pp. 694–699.

188. Gu, P.; Lee, W.-M.; Roubidoux, M.A.; Yuan, J.; Wang, X.; Carson, P.L. Automated 3D ultrasound image segmentation to aid breast cancer image interpretation. *Ultrasonics* **2016**, *65*, 51–58, doi:10.1016/j.ultras.2015.10.023.

189. Singh, B.K.; Verma, K.; Thoke, A.S. Fuzzy cluster based neural network classifier for classifying breast tumors in ultrasound images. *Expert Syst. Appl.* **2016**, *66*, 114–123, doi:10.1016/j.eswa.2016.09.006.

190. Shi, J.; Zhou, S.; Liu, X.; Zhang, Q.; Lu, M.; Wang, T. Stacked deep polynomial network based representation learning for tumor classification with small ultrasound image dataset. *Neurocomputing* **2016**, *194*, 87–94, doi:10.1016/j.neucom.2016.01.074.

191. Liu, J.; Zarshenas, A.; Wei, Z.; Yang, L.; Fajardo, L.; Suzuki, K.; Qadir, A. Radiation dose reduction in digital breast tomosynthesis (DBT) by means of deep-learning-based supervised image processing. In *Medical Imaging 2018: Image Processing*; International Society for Optics and Photonics: Bellingham, WA, USA, 2018; Volume 10574, p. 105740F.

192. Zou, L.; Yu, S.; Meng, T.; Zhang, Z.; Liang, X.; Xie, Y. A Technical Review of Convolutional Neural Network-Based Mammographic Breast Cancer Diagnosis. *Comput. Math. Methods Med.* **2019**, *2019*, 1–16, doi:10.1155/2019/6509357.

Publisher's Note: MDPI stays neutral with regard to jurisdictional claims in published maps and institutional affiliations.